STEADY STATE FLUID MODELS OF THE ION-EXOSPHERE

by

J. E. C. Gliddon and K. C. Yeh

NsG 24

November 1966

Sponsored by

National Aeronautics and Space Administration

Washington, D. C.

Electrical Engineering Research Laboratory

Engineering Experiment Station

University of Illinois

Urbana, Illinois

STEADY STATE FLUID MODELS OF THE ION-EXOSPHERE

by

J. E. C. Gliddon and K. C. Yeh

NsG 24

November 1966

Sponsored by

National Aeronautics and Space Administration

Washington, D. C.

Electrical Engineering Research Laboratory

Engineering Experiment Station

University of Illinois

Urbana, Illinois

STEADY STATE FLUID MODELS OF THE ION-EXOSPHERE

by

J. E. C. Gliddon* and K. C. Yeh

Department of Electrical Engineering

University of Illinois

Urbana, Illinois

TABLE OF CONTENTS

I. Introduction

II. Single-Fluid Hydromagnetic Equations

III. Statement of the Problem

IV. Adiabatic (Convective) Equilibrium

IV.1 Solution of the Equation of Motion along a Line of Force

IV.2 The Ring Current

IV.3 Distribution of Plasma Density along the Dipole Axis

IV.4 The Adiabatic Ion-Exosphere and the Theory of Whistler Propagation

IV.5 Instability Associated with Anisotropic Pressure

V. Isothermal (Conductive) Equilibrium

VI. Numerical Results

VI.1 Model Protonosphere

VI.2 Model Radiation Belt

VII. Discussion

Appendix A

References

---

*On leave of absence from Queen Mary College, University of London, London, England.

STEADY STATE FLUID MODELS OF THE ION-EXOSPHERE

Abstract

An ion-exosphere can be defined as the uppermost part of the ionosphere in which the self-collision time is much larger than the time required for ions to travel between mirroring points. In such a case the system is entirely controlled by the externally applied forces and the long-range Coulomb forces. If we assume that among these forces the Lorentz force is dominant and that the heat transport is negligible, a closed system of hydromagnetic equations can be derived by taking successive moments of the Vlasov equation. This system of equations is often referred to as the CGL theory or the double adiabatic theory. In this theory the two equations of state are equivalent to the requirement that the magnetic moment and the longitudinal invariant be adiabatic invariants.

The present investigation is concerned with the magnetohydrostatic solution of the CGL equations. The dilute plasma is assumed to be in a gravitational field, permeated by a strong dipole magnetic field and rotating with constant angular velocity about the dipole axis. These equations are solved in the dipole coordinate system by assuming that the ion-exosphere is either in adiabatic equilibrium or in isothermal equilibrium. Analytic expressions for the density, the elements of the pressure tensor, and the temperature of the fluid have been derived. A formula for the ring current has also been found. The results are illustrated by a number of representative curves.

STEADY STATE FLUID MODELS OF THE ION-EXOSPHERE

I. Introduction

The motion of charged particles in the Earth's magnetic field can be analyzed into three distinct cyclic motions. The first of these is the circular gyrating motion of a charged particle about a moving point called its guiding center. The period of gyration, sometimes known as the Larmor period, is approximately 1.5 micro-seconds for electrons and 2.8 milli-seconds for protons on the Earth's surface at the equator and increases as the third power of the radial distance from the center of the Earth. The second of the cyclic motions is the oscillatory motion of the particles along lines of force between their conjugate mirroring points. In this case, the guiding center of a particle oscillates with a period which depends on the energy of the particle, on the pitch angle of the particle in the equatorial plane, and on the particular line of force. For high-energy particles in the radiation belts, with energy 10 kev or higher, the period is a few seconds for electrons and about 100 seconds for protons (Van Allen, 1962; Akasofu and Chapman, 1961); for thermal particles the period approaches ten minutes for electrons and five hours for ions. Due to inhomogeneity of the field and the centrifugal force associated with motion along curved lines of force, the guiding center also drifts in longitude, electrons to the east and protons to the west. The time required in this third cyclic motion to drift once completely around the Earth is slightly more than three days for 10 kev electrons and ions and more than 100 years for thermal particles (Lew, 1961).

In general, plasmas can be classified as high density, medium density, or

low density, (Alfvén and Fälthammar, 1963). This classification depends largely on the magnitude of the self-collision time (Spitzer, 1956) as compared with the characteristic periods of the cyclic motions discussed in the preceding paragraph. When the self-collision time is shorter than the Larmor period, the velocity distribution is nearly isotropic and, hence, so are the transport coefficients. The effect of the magnetic field is felt only through the Lorentz force term $\underset{\sim}{J} \times \underset{\sim}{B}/c$ which, for example, renders the propagation of hydromagnetic waves anisotropic. When the self-collision time exceeds the Larmor period but is less than the mirroring period, all transport coefficients become highly anisotropic since now the transverse motion is restricted by the small Larmor radius while particles can move relatively freely in the longitudinal direction over a much larger distance. When the self-collision time is greater than the mirroring period, collisional effects can be ignored altogether. This condition may be expected to be satisfied for energetic particles in the Earth's environment above an altitude of some 1000 km, where the particles are predominantly electrons and protons. This region is defined as the ion-exosphere, (Eviator, et al., 1964). In this region the particles move only under the action of the applied field and the self-consistent field, and the transport coefficients in the ordinary sense may be meaningless. If such a plasma has existed over a period longer than the time required for a complete drift around the Earth, the plasma may then be said to have reached a steady state. It is in this context that the present theory is developed.

There is considerable interest at present in developing a theory for the protonosphere surrounding the Earth, (Dungey, 1955; Gliddon, 1963; Allen, et al., 1964; Angerami and Thomas, 1964). Of course the physical protonosphere

is very complex due to the presence of chemical reactions and dynamical motions of internal and external origins. In order to make the problem manageable, simplifying assumptions such as that of thermodynamic equilibrium and high density (so that pressure is isotropic and obeys the ideal gas law) have been made. The present low-density assumption represents the other extreme. The theory may be expected to apply to high energy particles and probably to the thermal particles in the protonosphere just beyond the discontinuity in electron density, known as the "knee", (Carpenter, 1963), which is believed to exist at a geocentric distance of some six Earth radii.

The paper is written according to the following brief outline.

Relevant equations are given in II and the problem is stated mathematically in III. In order to solve these equations two models have been considered. In the first model, the ion-exosphere is supposed to be in convective equilibrium. This may come about, for example, because of turbulence. It is further supposed that the mirroring period is so short that no appreciable conduction of heat can take place during one complete oscillation between conjugate mirroring points. As a result there is a tendency for adiabatic equilibrium to be set up. The solution of the adiabatic model and related discussions on ring current and instabilities are given in IV. In the second model the ion-exosphere is supposed to have existed so long that all temperature differences have been equalized and the ion-exosphere is then in isothermal equilibrium. This is discussed in V. It is interesting to remember that analogous situations exist in connection with the study of neutral atmospheric models (Mitra, 1952). As a matter of fact, even some of the theoretical difficulties are of the same nature. Using formulas derived in IV and V, numerical values

have been computed and the results are presented in VI. For each model, sample curves are shown for model protonosphere and model radiation belt. Finally the results of this investigation are discussed in VII.

II. The Single-Fluid Hydromagnetic Equations

We make use of the system of equations applicable to a dilute plasma permeated by a relatively strong magnetic field, (Chew, et al., 1956). In this theory collisions are ignored and the Lorentz force is assumed to be dominant in the Boltzmann equation. The procedure therefore is to assume that the velocity distribution function can be expanded in a series of ascending powers of m/e, where m is the mass and e the charge of an ion. It follows immediately that the first approximation to the distribution function must be axially symmetric in velocity space about a line parallel to the magnetic field B and hence the pressure tensor takes the form

$$\underset{\approx}{P} = P_{\perp} \underset{\approx}{I} + (P_{\parallel} - P_{\perp}) \underset{\sim}{b}\,\underset{\sim}{b} \quad , \tag{1}$$

where $\underset{\approx}{I}$ is the unit dyadic and $\underset{\sim}{b}$ is a unit vector parallel to $\underset{\sim}{B}$.

In terms of the mass density, ρ, mass velocity u, charge density q and current density J, the first and second moments of the Boltzmann equation yield, respectively, the equation of continuity

$$\frac{\partial \rho}{\partial t} + \operatorname{div} (\rho \underset{\sim}{u}) = 0 \quad , \tag{2}$$

and the equation of momentum transfer

$$\rho \frac{d\underset{\sim}{u}}{dt} = - \operatorname{div} \underset{\approx}{P} - \rho \operatorname{grad} \phi + q \underset{\sim}{E} + \frac{1}{c} (\underset{\sim}{J} - q\underset{\sim}{u}) \times \underset{\sim}{B} \quad , \tag{3}$$

where ϕ is the potential due to body force. Mixed Gaussian units are used here.

An equation of state can be found by taking the third moment of the

Boltzmann equation, but this introduces a new tensor representing heat transport. The system of equations can be closed if it is assumed that heat transport can be ignored. In this case the third moment-equation provides two adiabatic relations

$$\frac{d}{dt} \left(P_{\parallel} B^2/\rho^3\right) = 0 \tag{4}$$

and

$$\frac{d}{dt} \left(P_{\perp} /\rho B\right) = 0 \ . \tag{5}$$

We shall assume that these relations are a sufficiently good approximation for use in our model. Equation (5) is evidently the analogue of the adiabatic invariant magnetic moment of a single charged particle. It can be shown that equation (4) when combined with equation (5) is equivalent to the condition of longitudinal invariant (Thomson, 1962). Since this paper solves only for the steady state solution, it implies that all three adiabatic invariants must hold.

To the first approximation, the CGL theory requires the electric field $\underset{\sim}{E}$ to satisfy the condition appropriate to a fluid of infinite conductivity,

$$\underset{\sim}{E} + \frac{1}{c} \underset{\sim}{u} \times \underset{\sim}{B} = 0 \ . \tag{6}$$

The electromagnetic variables also satisfy Maxwell's equations which, for our case, are

$$\text{curl } \underset{\sim}{E} = 0 \ , \tag{7}$$

$$\text{curl } \underset{\sim}{B} = \frac{4\pi}{c} \underset{\sim}{J} \ , \tag{8}$$

$$\text{div } \underset{\sim}{E} = 4\pi q \ , \tag{9}$$

$$\text{div } \underset{\sim}{B} = 0 \ . \tag{10}$$

The problem we consider is that of a plasma rotating steadily with angular velocity ω about the axis of a magnetic dipole. The plasma is acted upon by a gravitational force directed towards the dipole. Now a rotational velocity-field automatically satisfies equation (2). Also, the electric field is determined by equation (6) and equation (7) restricts ω to a constant value on any one line of force (Ferraro, 1937). Equation (9) then implies the presence of a charge distribution q, which dimensional arguments (Dungey, 1958) show, is extremely small in the infinite conductivity approximation. The terms involving q in equation (3) can thus be neglected. The problem therefore reduces to the determination of the unknows ρ, $\underset{\sim}{P}$ and $\underset{\sim}{J}$ from equations (3), (4), and (5). The remaining equations (6) and (8), which have not so far been referred to, serve to determine the perturbation magnetic field due to the current density $\underset{\sim}{J}$.

III. Statement of the Problem

A dipole of moment M_0 is situated at the origin of a fixed coordinate system with its axis directed along the z-axis. Plasma is assumed to be rotating steadily with angular velocity ω (constant along any given line of force) about the axis of the dipole. At distances two to five Earth radii, the rotational force is small and therefore the equations will be given in the non-rotating coordinate system. The coordinates of any point in the plasma may be referred to (see figure in Appendix A) by the spherical polar coordinates (r, θ, ϕ) or by the dipole coordinates (x^1, x^2, x^3), details of which are given in the Appendix. The equation of motion,

$$\rho \frac{d\underset{\sim}{u}}{dt} = - \text{div } \underset{\approx}{P} - \rho \text{ grad } \phi + \frac{1}{c} \underset{\sim}{J} \times \underset{\sim}{B} , \tag{11}$$

has the following components parallel respectively to the x^1, x^2, x^3 dipole coordinate lines:

$$\frac{\partial P_{\parallel}}{\partial x^1} + (P_{\parallel} - P_{\perp}) \frac{\partial \ln h_2 h_3}{\partial x^1} + \rho h_1 \left[\frac{GM}{r^2} \sin I - \omega^2 r \sin\theta \cos(\theta - I)\right] = 0 , \tag{12}$$

$$J_3 = - \frac{c}{B}\left[\frac{1}{h_2} \frac{\partial P_{\parallel}}{\partial x^2} + \frac{P_{\perp} - P_{\parallel}}{h_2} \frac{\partial \ln h_1}{\partial x^2} + \frac{\rho GM}{r^2} \cos I - \omega^2 \rho r \sin\theta \sin(\theta - I)\right] , \tag{13}$$

$$J_2 = \frac{c}{B}\left[\frac{1}{h_3} \frac{\partial p_{\perp}}{\partial x^3} + \frac{P_{\parallel} - P_{\perp}}{h_3} \frac{\partial \ln h_1}{\partial x^3}\right] = 0. \tag{14}$$

In the above equations ϕ has been replaced by $-GM/r$ where G is the gravitational constant and M is the mass of the Earth. We see from equation (12)

that there is need of relations relating ρ and $P_\perp$ to $P_{||}$. Since we are only seeking steady-state solutions and the fluid is assumed to have only rotational motion, equations (4) and (5) indicate that $P_{||}B^2/\rho^3$ and $P_\perp/\rho B$ are independent of x^3 but may be arbitrary functions of x^1 and x^2. Therefore, it seems that the description of the problem is still incomplete, unless additional conditions are imposed. Actually the situation is analogous to the study of a neutral atmosphere (Mitra, 1952). Following this analogy, we consider an adiabatic and an isothermal model. For the adiabatic model, it is sufficient to assume that the quantities $P_{||}B^2/\rho^3$ and $P_\perp/\rho B$ are constant along a line of force.

Therefore, the end conditions we use, for the adiabatic model, are

$$P_{||} = P_\perp = P_0$$

$$\rho = \rho_0 \qquad (15)$$

and

$$B = B_0 ,$$

at the point (r_0, θ_0) on the line of force where it leaves the ion-exosphere and enters the region where collisions become sufficiently frequent to secure isotropy of pressure. This region extends over a height range of the order of a scale height which is small when compared with the length of the field line. Therefore, such a boundary condition may not be too unreasonable to use. Actually isotropy of pressure is not a limitation in the present theory, but only an assumption which simplifies the final formulas. The quantities with suffix zero are assumed to be known. The adiabatic relations, expressed in terms of the end conditions, are

$$P_{\parallel} B^2/\rho^3 = P_0 B_0^2/\rho_0^3 = c_{\parallel} , \tag{16a}$$

and

$$P_{\perp}/\rho B = P_0/\rho_0 B_0 = c_{\perp} , \tag{16b}$$

where $c_{\parallel}$ and $c_{\perp}$ are known constants for any given line of force.

For the isothermal ion-exosphere equations (16a) and (16b) must be replaced by the assumption of equal temperatures

$$P_{\parallel}/\rho = P_{\parallel 0}/\rho_0 = K_{\parallel} \tag{17a}$$

and

$$P_{\perp}/\rho = P_{\perp 0}/\rho_0 = K_{\perp} \tag{17b}$$

where again $K_{\parallel}$ and $K_{\perp}$ are known constants for any given line of force.

The use of either equations (16) or (17) will make equation (12) an ordinary first order differential equation, expressing the variation of P along a line of force. The equation is then solved for each model in IV and V, subject to the respective end conditions.

IV. Adiabatic Equilibrium

In an adiabatic ion-exosphere, equations (16a) and (16b) are valid. When they are substituted into equation (12) $P_{//}$ can be solved.

IV.1 Solution of the Equation of Motion along a Line of Force

Consider a line of force whose equation is

$$R = L \sin^2 \theta \quad , \tag{18}$$

where $R = r/r_0$ and $r_0 L$ is the geocentric distance of the point where the line of force cuts the equatorial plane. The number L is known as the L-shell number, but normalized by a geocentric radius to the base of the ion-exosphere. Using (16) and (17) to eliminate $P_{\perp}$ and ρ, we may express equation (12) in the form

$$\frac{dP_{//}}{dR} + \frac{24L-15R}{2R(4L-3R)} P_{//} + \left[-k_1 \frac{(24L-15R)}{R^6(4L-3R)^{1/6}} + k_2 \frac{(4L-3R)^{1/3}}{R^4} - k_3(4L-3R)^{1/3}\right] P_{//}^{1/3} = 0 \tag{19}$$

where

$$k_1 = c\, M_0^{5/3}/2c^{1/3} L^{5/6} r_0^5 \quad ,$$

$$k_2 = GMM_0^{2/3}/c^{1/3} L^{1/3} r_0^3 \quad ,$$

and

$$k_3 = 3M_0^{2/3}\,\omega^2 / 2c_{//}^{1/3} L^{4/3} \tag{20}$$

Equation (19), which is of the Bernoulli type, can be integrated without difficulty. The solution of the problem can then be conveniently expressed by the formulas

$$P_{//}/P_0 = (B/B_0)\,\Delta^{3/2} , \tag{21}$$

$$P_{\perp}/P_0 = (B/B_0)^2\,\Delta^{1/2} , \tag{22}$$

$$\rho/\rho_0 = (B/B_0)\,\Delta^{1/2} , \tag{23}$$

where

$$\Delta = \frac{5}{3} - \frac{2}{3}\frac{B}{B_0} + \frac{r_0}{3H_0}\left(\frac{1}{R} - 1\right) + \frac{\omega^2 \rho_0 r_0^2}{3P_0 L}\left(R^3 - 1\right) \tag{24}$$

and

$$H_0 = P_0/(2GM\rho_0 r_0^{-2}) \tag{25}$$

is the scale height of the plasma at the end-point of the line of force (distance r_0 from the center of the Earth).

Temperature has not so far been defined for the fluid model. We may define a temperature θ by means of the equation

$$\frac{3}{2}\, n\, \theta = \frac{1}{2}\left(P_{//} + 2P_{\perp}\right) , \tag{26}$$

which yields the expression

$$\frac{\theta}{\theta_0} = \frac{1}{9}\left[5 + 4B/B_0 + (r_0/H_0)\left(\frac{1}{R} - 1\right) + \frac{\omega^2 \rho_0 r_0^2}{P_0 L}\left(R^3 - 1\right)\right] . \tag{27}$$

On the other hand, it may be meaningful to define separate temperatures $\theta_{\parallel}$ and $\theta_{\perp}$, corresponding respectively to $P_{\parallel}$ and $P_{\perp}$; thus if

$$\frac{3}{2} n \theta_{\parallel} = \frac{1}{2} P_{\parallel} , \qquad \frac{3}{2} n \theta_{\perp} = P_{\perp} , \tag{28}$$

the parallel and perpendicular temperature ratios are given by, respectively,

$$\frac{\theta_{\parallel}}{\theta_0} = \frac{1}{3} \Delta , \qquad \frac{\theta_{\perp}}{\theta_0} = \frac{2B}{3B_0} . \tag{29}$$

IV.2 The Ring Current

In order to support the fluid hydrostatically currents must flow in the ion-exosphere. Due to symmetry of the problem the current along the equipotential coordinate line vanishes as shown by equation (14). The azimuthal current in the form of a filamentary ring current is given by equation (13). This current can be re-expressed by using the metric coefficients given in the Appendix but the resulting expression is too complex to be of value. It we assume that the end conditions be uniform over the globe, the current density in the equatorial plane can be shown to be

$$J_3 = \frac{c P_{\perp E}}{r_0 B_E} \left\{ \frac{4}{4L-3} + \frac{B_0}{B_E} \left[\frac{5}{L} + \frac{r_0}{H_0 L} \left(\frac{1}{2L} - 1 \right) + \frac{\omega^2 \rho_0 r_0^2}{P_0 L^2} (2L^3 - 1) \right] \right.$$

$$\left. - \frac{1}{2 \Delta_E} \left[\frac{24L-15}{3L^5 (4-3/L)^{3/2}} - \frac{r_0}{3H_0 L^2} + \frac{\omega^2 \rho_0 r_0^2}{3P_0} (2L + 1/L^2) \right] \right\} , \tag{30}$$

where the subscript E is used to denote the quantity referred to the equatorial plane.

Several numerical examples of interest are given in Section VI.

IV.3 Distribution of Plasma Density along the Dipole Axis

Formulas (21)-(23) take a simpler form when we consider variations along the polar line of force. The density ratio, for example, becomes

$$\frac{\rho_p}{\rho_0} = \frac{1}{R^3}\left[\frac{5}{3} - \frac{r_0}{3H_0} + \frac{r_0}{3H_0 R} - \frac{2}{3R^3}\right]^{1/2} \tag{31}$$

where ρ_p stands for plasma density on the polar line. It should be mentioned that there are complications in the case of the polar line. Because of infinite length of the line of force, collisional effects, as well as the possibility of escape, must be taken into account. In addition, consideration of the expression inside the square bracket of (31) shows that H_0 must exceed $r_0/5$ if the density and pressure are to remain positive everywhere on the polar line. An alternative statement of this condition is that at the base of the ion-exosphere the total thermal energy of electrons and ions must exceed three-fifths of the ion gravitational energy in order for the pressures and the density to remain positive. Since the CGL theory assumes that the Lorentz force is dominant the gravitational force should not be too large for the theory to remain valid.

Taking $r_0 = 7 \times 10^8$ cm, we find that if

$$T_{i0} + T_{e0} > 2800^{\circ}K$$

at the base of the exosphere, the density and pressure will remain positive everywhere.

It is worth noting that similar difficulties also appear in the adiabatic neutral atmosphere (Mitra, 1952). There the neutral scale height H_0 must exceed $(\gamma-1)\gamma_0/\gamma$ in order for the density to remain positive even at infinity. The quantity γ is the ratio of specific heats. The usual explanation is that the highly idealized adiabatic model may be expected to apply only in the troposphere or below, where the theory predicts a correct behaviour when ground values are used as end conditions.

IV.4 The Adiabatic Ion-Exosphere and the Theory of Whistler Propagation

The study of plasma density (or pressure) in the equatorial plane as a function of the conditions existing at the base of the ion-exosphere can be simplified by carrying out approximations to the quantity Δ appearing in equations (21)-(23). The second term in equation (24) becomes negligible when $R > 2$, at least as a first approximation. Again, the last term in equation (24) which represents the effect of the rigid body rotation, is negligible for values of R such that $2 \leq R \leq L < 5$. Thus we can write

$$\frac{\rho}{\rho_0} = \frac{B}{B_0}\left[\frac{5}{3} - \frac{r_0}{3H_0}\left(1 - \frac{1}{R}\right)\right]^{1/2}, \quad (2 < R \leq L < 5), \tag{32}$$

where

$$\frac{B}{B_0} = \frac{1}{R^3}\left(\frac{4L - 3R}{4L - 3}\right)^{1/2}. \tag{33}$$

The density distribution ρ_E on the equatorial plane is obtained by writing $R = L$,

$$\frac{\rho_E}{\rho_0} \approx \frac{1}{L^3}\left(\frac{L}{4L - 3}\right)^{1/2}\left[\frac{5}{3} - \frac{r_0}{3H_0}\left(1 - \frac{1}{L}\right)\right]^{1/2}, \quad (2 < R \leq L < 5). \tag{34}$$

We can now consider the effect on ρ_E when ρ_0 and H_0 vary with latitude. If ρ_0 is an increasing function of L (ρ_0 increasing in the direction from equator to pole) it is obvious from equation (34) that ρ_E will decrease more slowly than it would if ρ_0 had a constant value. Again, if H_0 (or equivalently, the temperature) at the reference level is an increasing function of L, the value of the expression in square brackets in equation (34) also increases and hence, in this case also, ρ_E decreases more slowly with altitude. Observation of whistlers has led to the suggestion that the plasma density in the equatorial plane may decrease rather abruptly between three and four Earth radii. According to the fluid model, such a decrease would be consistent with an increase in plasma temperature or a decrease in plasma density (or both) at the base of the ion-exosphere between approximate geomagnetic latitudes 55° and 60°.

A simple relationship $\rho \propto B$ (along a given line of force) has been suggested (Storey, 1953; and Smith, 1961) as being consistent with whistler theory. The time delay T for a one-way travel of a whistler signal along a line of force can be calculated from the well-known formula

$$T = \frac{1}{2cf} \int \frac{f_p}{f_H} \left(1 - \frac{f}{f_H}\right)^{-3/2} ds \qquad (35)$$

where f is the frequency of the signal, f_p is the plasma frequency, f_H is the gyrofrequency for electrons, c is the velocity of light and ds is the element of arc of the line of force. Figure 1 shows the time-delay curves calculated for various lines of force, assuming in equation (35) that the electron density is directly proportional to B along each line of force and that the number density at the base of the ion-exosphere is 2×10^4/cc. The curves are

certainly qualitatively consistent with observed time-delay curves. In particular, the curve for L = 5 reproduces the phenomenon of a minimum time delay known as the nose whistler. It appears that no justification has been advanced in support of the law $\rho \propto B$ and some authors consider it cannot be justified. Dungey (1962) claims that the approximation is implausible. His argument is based on a particular case of a more general pitch-angle distribution function derived by Parker (1957). The adiabatic fluid model certainly suggests that $\rho \propto B$ may be a rough approximation, as shown in Section VI.1, even though the CGL theory may apply more appropriately to belts of high-energy particles rather than to background particles.

IV.5 Instability Associated with Anisotropic Pressure

We have given the adiabatic solution of the problem in (21)-(23). The next question to ask is whether the given solution is stable to small perturbations. While the complete answer to this question is unavailable, it is of interest to examine whether instability may arise due to anisotropic pressure. Such instability may arise as follows: if the magnetic field is adiabatically distorted so that the curvature is increased locally, the particles following the lines of force with velocity corresponding to temperature $\theta_{\parallel}$ will experience an increased centrifugal force. If the sum of the magnetic pressure and the perpendicular particle pressure is not large enough to balance the centrifugal force, the perturbation will grow. By obvious analogy, this instability is usually referred to as the "garden-hose" instability. The condition for this type of instability to occur in a homogeneous collisionless plasma is, (Parker, 1958)

$$P_{\parallel} > P_{\perp} + B^2/4\pi \quad . \tag{36}$$

Along a given line of force this inequality would be satisfied first at points in the equatorial plane. It will be sufficient for our purposes, therefore, to determine where (36) is satisfied in the equatorial plane. Using the subscript E to denote the equatorial quantities, (36) can be rewritten as

$$B_0^2/(4\pi\ P_0) < \frac{(P_{\parallel E} - P_{\perp E})/P_0}{(B_E/B_0)^2} \quad . \tag{37}$$

This equation indicates that the plasma is unstable if the ratio of the magnetic pressure to the particle pressure at the base of the ion-exosphere is less than the ratio of the normalized difference in equatorial particle pressures to the normalized equatorial magnetic pressure. The formula (37) enables us to determine the critical number-density n_0^* at the base of the ion-exosphere such that if $n_0 > n_0^*$ the garden-hose instability will occur. The critical number-density so defined is given by

$$n_0^* = \frac{B_0^2/4\pi}{kT_0\ \Delta_E^{1/2}\ [L^3\ \Delta_E(4-3/L)^{1/2} - 1]} \tag{38}$$

where Δ_E is the equatorial value of Δ given by equation (24).

Two cases are considered and the results are shown in Figure 2. In the first case, the average of electron and ion temperature T_0 at the base of the ion-exosphere is assumed to be $1500^{\circ}K$, corresponding to thermal particles. In the second case, a temperature appropriate for particles of 10 kev energy is used. This case may be considered to represent a belt of high-energy particles. Instability occurs at any L value if the number-density n_0 at the

of the ion-exosphere exceeds the value of n_0^* indicated on the graphs. For the thermal case, it can be seen that if n_0 is 10^5 or less the ion-exosphere is stable against the garden-hose instability. If n_0 is 10^6, instability appears for $L \geq 24$. For the high-energy belt case, instability can occur, for example, at $L = 6$ if n_0 exceeds 10^3.

The kind of instability considered here has received detailed treatment by Noerdlinger (1963) who shows (again for uniform plasma) that the wave-number of the fastest growing waves is of the order of $0.1\ \omega_p/c$. At a distance of three Earth radii this gives a wave-number of about 10^{-5} cm^{-1}, corresponding to a wavelength of 6×10^5 cm. This is very small when compared with an Earth radius of 6×10^8 cm, a distance over which most quantities vary significantly. It seems permissible therefore to use the instability criterion, developed for uniform plasma, as a rough guide in the present discussion.

V. Isothermal Equilibrium

In an isothermal atmosphere equations (17a) and (17b) are valid. When they are substituted into equation (12) the following differential equation is obtained.

$$\frac{dP_{\parallel}}{dR} + \left[\frac{3(8L - 5R)}{2R(4L - 3R)}\left(1 - \frac{K_{\perp}}{K_{\parallel}}\right) + \frac{1}{K_{\parallel}}\left(\frac{GMr_0}{R^2} - \frac{3\omega^2 R^2}{L}\right)\right] P_{\parallel} = 0 \quad . \tag{39}$$

Equation (39) can be integrated easily to yield, along the line of force,

$$\frac{P_{\parallel}}{P_{\parallel 0}} = \frac{P_{\perp}}{P_{\perp 0}} = \frac{\rho}{\rho_0} = \left(\frac{B}{B_0}\right)^{1-P_{\perp 0}/P_{\parallel 0}} \exp\left[\frac{r_0}{H_0'}\left(\frac{1}{R} - 1\right) + \frac{\omega^2 \rho_0 r_0^2}{2P_0 L}\left(R^3 - 1\right)\right] \quad . \tag{40}$$

The scale height H_0' is by definition

$$H_0' = P_{\parallel 0} r_0^2 / GM\rho_0 = 6\,\theta_{\parallel 0}/mg_0 \quad , \tag{41}$$

which differs from that defined earlier in equation (25).

For the special case $P_{\perp 0} = P_{\parallel 0} = P_0$ and negligible rotational effect, equation (40) reduces to

$$P/P_0 = \rho/\rho_0 = \exp\left[r_0(1/R - 1)/H_0'\right] \quad , \tag{42}$$

an expression which can be derived by using the usual fluid collision dominated model with a scalar pressure. The result of equation (24) shows that even in the collisionless case the pressure for an isothermal ion-exosphere is a scalar everywhere along a field line if it is so at the end of the line. Now sine $P_{\parallel} = P_{\perp} = P$ everywhere along the line of force, equation (36) can never be satisfied and hence there is no garden-hose instability. If the pressure at the end of the field line is allowed to be anisotropic,

instability will arise only if $P_{\parallel 0} > P_{\perp 0}$.

It is interesting to note that an equation identical in form with equation (42) applies to the isothermal neutral atmosphere (Mitra, 1952). The only differences are in the definition of scale height and in the fact that equation (42) applies along the magnetic lines of force while in the neutral atmosphere it applies along a radial line. As in the case of the neutral atmosphere, equations (40) and (41) give positive values of P and ρ even when R approaches infinity along the polar line.

VI. Numerical Results

The theory developed in this paper will be used to study two models: (1) model protonosphere and (2) model radiation belt. In the first case we have the background thermal particles in mind, while in the second case we study the effect of a hypothetical belt of high-energy particles such as that considered by Akasofu and Chapman (1961). The theory applies more appropriately to high-energy particles than to thermal particles. In view of the present lack of a valid theory, the first model study is presented only for comparison purposes.

The following numerical values apply to both models:

$$G = 6.7 \times 10^{-8} \text{ dyne cm}^2 \text{ g}^{-2} \qquad \omega = 7.27 \times 10^{-5} \text{ rad sec}^{-1}$$

$$M = 6 \times 10^{27} \text{ g(mass of Earth)} \qquad M_0 = 8.19 \times 10^{25} \text{ gauss cm. (dipole moment)}$$

$$m = 1.7 \times 10^{-24} \text{ g(mass of proton)} \quad r_0 = 7 \times 10^{8} \text{ cm } (\approx 1.1 \text{ Earth radii})$$

$$k = 1.4 \times 10^{-16} \text{ erg deg}^{-1} \text{ (Boltzmann's constant).} \tag{43}$$

For purposes of computation we assume that the base of the ion-exosphere is at a height of approximately one tenth of an Earth radius. For the adiabatic model it is convenient to assume that at the base of the ion-exosphere collisions are sufficiently numerous to render the distribution function isotropic. This assumption is relaxed in the isothermal model in order to allow the study of effects caused by anisotropic pressure at the base. Other numerical values appropriate to each model will be given in the following subsections.

VI.1 Model Protonosphere

In addition to the numerical values given in (43) we shall assume the sum of electron and ion temperatures at the base of the ion-exosphere to be $3000^{o}K$ over the whole globe. These data suffice to compute the ratios $P_{\parallel}/P_{0}$, $P_{\perp}/P_{0}$, ρ/ρ_{0}, and θ/θ_{0} along any line of force for an adiabatic model.

In Figure 3 the variation of each ratio as a function of R is displayed for various lines of force (that is, for various values of L). Also shown on Figures 3a and 3b, for comparison, are the graph of B/B_{0} and curves of number-density ratios (N/N_{0}) computed (by a completely different method) by Eviator, et al. (1964). It will be noted that the plasma density along a line of force is quite closely proportional to the magnetic field strength B and this property was used in Section IV.4 to compute whistler time-delay. It is also interesting to note that the present theory predicts a plasma density consistently greater than the corresponding densities computed from the Eviator, et al. (1964) model.

Plots similar to those in Figure 3 have also been made for an isothermal protonosphere. These are shown in Figures 4a, 4b, and 4c for L = 1.5, 3 and 6 respectively. In each case the possibility that the pressure may be anisotropic at the base of ion-exosphere is also considered by allowing $b = P_{\perp 0}/P_{\parallel 0}$ to take values 0.8, 1.0 and 1.2. It is interesting to note that for $b > 1$, the curves may have a minimum. This comes about because $(B/B_{0})^{1-b}$ increases with R while the exponential factor in equation (40) decreases with R. In addition to the numerical values given in (43) we have also assumed that $T_{\parallel 0} = 500^{o}K$, $P_{\parallel 0} = 8.28 \times 10^{-9}$ g/cm-sec^{2} so that the scale height H_{0}' comes out to be 3.06×10^{8} cm.

Comparison of Figure 3 with Figure 4 shows that in general the pressure

and density in an adiabatic model decreases faster than in the corresponding isothermal model.

The variation of proton density-ratio with latitude at fixed heights in an adiabatic model is plotted in Figure 5. These curves show that if the ion density and temperature at the base of the ion-exosphere are constant (independent of latitude) then the ion density at fixed heights increases from a minimum at the equator to a maximum at the poles. The same latitude-dependence is to be seen in the similar graphs drawn by Eviator, et al. (1964) and is attributable to the anisotropy introduced by the geomagnetic field.

In order to compute the current density we further assume the number-density at the base of the ion-exosphere to be 2×10^4 electrons/cc. The results are shown in Figures 6 and 7. Figure 6 shows the current density in the equatorial plane and it is seen that the current decreases monotonically as L increases. The current density along a few sample L-shells is shown in Figure 7. We see that the current density along the line of force reaches a minimum between the base of the ion-exosphere and the equator. It is interesting to note that these filamentary ring currents flow in the positive x^3-axis (westward) direction and hence display the diamagnetic effect. The Earth's main magnetic field is weakened slightly as a result. The curves shown in Figures 6 and 7 are computed only for the adiabatic model. Similar curves can be computed for the isothermal model without difficulty.

VI.2 Model Radiation Belt

In case the particles have energies of order kev or higher the formulas (24) and (40) can be simplified since the gravity effect and the rotation

effect may be ignored. For the adiabatic model we obtain from equation (24)

$$\Delta = (5 - 2B/B_0)/3 \quad . \tag{44}$$

When equation (44) is substituted into (21), (22), (23) and (29) the pressure ratio, density ratio and temperature ratio can be computed. Note that these ratios now depend only on the magnetic field. Sample curves showing the variation of pressure, density and temperature are depicted in Figure 8 for magnetic lines of force L = 1.5, 3 and 6. It will be noted that $\theta_{\parallel}$ increases with R. This is the reverse of the behavior of $\theta_{\parallel}$ observed in the model protonosphere. The difference is due to the fact that gravity is unimportant in the radiation belt model.

Similar simplification also applies to the isothermal radiation belt. Equation (40) reduces simply to

$$P_{\parallel}/P_{\parallel 0} = (B/B_0)^{1-P_{\perp 0}/P_{\parallel 0}} \quad . \tag{45}$$

Equation (45) shows that in an isothermal radiation belt pressure and density are uniform everywhere along the line of force if the pressure is isotropic at the end of the field line. In case the pressure is not isotropic at the end, the variation of pressure and density along the lines of force corresponding to L = 1.5, 3, and 6 has been computed and is shown in Figure 9. By comparing Figure 8 with Figure 9 the differences between the adiabatic and isothermal models can be easily observed.

As a last example we consider the hypothetical belt inferred by observations of auroral phenomenon. Here, instead of values at the base of ionexosphere we shall assume the values at the equator are known. Following

Akasofu and Chapman, the equatorial number density is assumed to have a gaussian form,

$$n_E = \exp[-g^2(L - L_0^2)] \tag{46}$$

The center of the belt is at $L_0 = 6$ and the value of g is 1.517. Since the energies of these particles are very high the simplified form indicated by equation (44) is used. The computations have been made for the adiabatic model and the results are illustrated in Figure 10 as contour plots. Figure 10a shows constant $P_{||}$ curves in polar coordinates. The belt nature is obvious. A similar plot for $P_{\perp}$ is shown in Figure 10b. Comparison of Figure 10a and Figure 10b indicates again that $P_{\perp}$ decreases along the line of force more rapidly than does $P_{||}$. The mass density contours are shown in Figure 10c and the current density contours are shown in Figure 10d.

The current density is computed directly from equation (13). Because of the presence of transverse gradient of $P_{||}$ term and the gaussian nature of the belt, eastward current flows for R less than about 3 as shown in Figure 10d. For R larger than about 3, $P_{||}$ has decreased sufficiently so that the curvature term would dominate and as a result the current flows westward.

VII. Discussion

We have presented magnetohydrostatic solutions of the CGL theory in a dipole coordinate system. Analogous to neutral atmospheric theory both adiabatic and isothermal models have been considered. The CGL equations used completely ignore effects of collisions. For the adiabatic model, this is equivalent to requiring validity of all three adiabatic invariants. For the isothermal model, the solution reduces to the case obtained for the collision dominated plasma.

The actual behavior of the magnetosphere is probably somewhere between the adiabatic model and the isothermal model considered in this paper. If the temperature along the line of force is measured or inferred from other theoretical considerations so that $K_{\parallel}$ and $K_{\perp}$ are known, equation (39) can be integrated to obtain a more realistic model.

Appendix A

The scalar potential V for a dipole of moment M_0, situated at the origin O with its axis directed along the z-axis is given by

$$V = (M_0 \cos \theta)/r^2 \qquad (AA.1)$$

The magnetic induction $B = |\text{grad } V|$ and the "angle of dip" I between the direction of the magnetic field and the horizontal and hence given respectively by

$$B = \frac{M_0}{r^3} (1 + 3 \cos^2 \theta)^{1/2} \qquad (AA.2)$$

and

$$\tan I = 2 \cot \theta \ . \qquad (AA.3)$$

Dipole coordinates (x^1, x^2, x^3) are defined by the line of force, the equipotential curve and the circle of latitude through any given point. The coordinate lines are given by

$$\begin{aligned} &\text{line of force, } r = x^2 \sin^2 \theta \ , \\ &\text{equipotential line, } r^2 = x^1 \cos \theta \ , \\ &\text{circle of latitude, } \phi = -x^3 \end{aligned} \qquad (AA.4)$$

The squared element of arc in the dipole coordinate system is given by

$$ds^2 = (h_1 dx^1)^2 + (h_2 dx^2)^2 + (h_3 dx^3)^2$$

where the metric coefficients have the values

$$h_1^2 = \frac{\cos^4\theta}{r^2(1 + 3\cos^2\theta)} , \quad h_2^2 = \frac{\sin^6\theta}{1 + 3\cos^2\theta} , \quad h_3^2 = r^2\sin^2\theta \ . \tag{AA.5}$$

If $\underset{\approx}{P}$ is the tensor defined by equation (1), the physical components of div $\underset{\approx}{P}$ in the curvilinear coordinate system are

$$(\text{div } \underset{\approx}{P})_1 = \frac{1}{h_1}\left[\frac{\partial P_{\parallel}}{\partial x^1} + (P_{\parallel} - P_{\perp})\frac{\partial}{\partial x^1}(\ln h_2 h_3)\right] \tag{AA.6}$$

$$(\text{div } \underset{\approx}{P})_2 = \frac{1}{h_2}\left[\frac{\partial P_{\perp}}{\partial x^2} + (P_{\perp} - P_{\parallel})\frac{\partial}{\partial x^2}(\ln h_1)\right] \tag{AA.7}$$

$$(\text{div } \underset{\approx}{P})_3 = \frac{1}{h_3}\left[\frac{\partial P_{\perp}}{\partial x^3} + (P_{\perp} - P_{\parallel})\frac{\partial}{\partial x^3}(\ln h_1)\right] \tag{AA.8}$$

We are essentially concerned with transformations from the variables (x^1, x^2) to the variables (r, θ). By differentiating the first two of equations (AA.4) we obtain the transformations

$$\frac{\partial}{\partial x^1} = \frac{2\cos^3\theta}{r(1 + 3\cos^2\theta)}\frac{\partial}{\partial r} + \frac{\cos^2\theta\sin\theta}{r^2(1 + 3\cos^2\theta)}\frac{\partial}{\partial\theta} \tag{AA.9}$$

$$\frac{\partial}{\partial x^2} = \frac{\sin^4\theta}{1 + 3\cos^2\theta}\frac{\partial}{\partial r} - \frac{2\sin^3\theta\cos\theta}{r(1 + 3\cos^2\theta)}\frac{\partial}{\partial\theta} \tag{AA.10}$$

Any function $f(r,\theta)$ becomes a function of θ only, or of r only, on a given line of force. In this case we may write

$$\frac{\partial f}{\partial x^1} = \frac{\cos^2\theta\sin\theta}{r^2(1 + 3\cos^2\theta)}\frac{df}{d\theta} = \frac{2}{r}\frac{\cos^3\theta}{1 + 3\cos^2\theta}\frac{df}{dr} \tag{AA.11}$$

The derivatives of metric coefficients occurring in (AA.6) and (AA.7) are given by

$$\frac{\partial}{\partial x^1}(\ln h_2 h_3) = \frac{\cos^3\theta(9 + 15\cos^2\theta)}{r^2(1 + 3\cos^2\theta)^2} \qquad \text{(AA.12)}$$

$$\frac{1}{h_1 h_2}\frac{\partial h_1}{\partial x^2} = \frac{3\sin\theta(1 + \cos^2\theta)}{r(1 + 3\cos^2\theta)^{3/2}} \,. \qquad \text{(AA.13)}$$

References

Akasofu, S. I. and Chapman, S., "The Ring Current, Geomagnetic Disturbance, and the Van Allen Radiation Belts," J. Geophys. Res., 66, 1321, 1961.

Alfvén, H. and Fälthammer, C-G., Cosmical Electrodynamics, Second Edition, Oxford, Chapter 5, 1963.

Allen, J. E., Segre, S. E., and Turrin, A., "The Disposition of an Ionized Gas in a Gravitational Field," II Nuovo Cimento, 31, 402, 1964.

Angerami, J. J. and Thomas, J. O., "Studies of Planetary Atmospheres, 1, The Distribution of Electrons and Ions in the Earth's Exosphere," J. Geophys. Res., 69, 4537, 1964.

Carpenter, D. L., "Whistler Evidence of a 'Knee' in the Magnetospheric Ionization Density Profile," J. Geophys. Res., 68, 1675, 1963.

Chew, G. F., Goldberger, M. L., and Low, F. E., "The Boltzmann Equation and the One-Fluid Hydromagnetic Equations in the Absence of Particle Collisions," Proc. Roy. Soc., A236, 112, 1959.

Dungey, J. W., "Physics of the Ionosphere," The Physical Society, London, 229, 1955, Cosmic Electrodynamics, C.U.P., 1958, in Geophysics, "The Earth's Environment," Ed. DeWitt, Gordon and Breach, New York, 1962.

Eviator, A., Lenchek, A. M., and Singer, S. F., "Distribution of Density in an Ion-Exosphere of a Non-Rotating Planet," Phys. Fluids, 7, 1775, 1964.

Ferraro, V. C. A., "Non-Uniform Rotation of the Sun and Its Magnetic Field," Mon. Not. Roy. Astron. Soc., 97, 458, 1937.

Gliddon, J. E. C., "The Distribution of Ions in the Exosphere," J. Atmos. Terr. Phys., 27, 175, 1963.

Lew, J. S., "Drift Rate in a Dipole Field," J. Geophys. Res., 66, 2681, 1961.

Mitra, S. K., "The Upper Atmosphere," The Asiatic Society, Calcutta, Second Edition, 1952.

Noerdlinger, P. D., "Growing Transverse Waves in Plasma in Magnetic Field," Annals of Physics, 22, 12, 1963.

Parker, E. N., "Newtonian Development of the Dynamical Properties of Ionized Gases of Low Density," Phys. Rev., 107, No. 4, 924, 1957, "Dynamical Instability in an Anisotropic Gas of Low Density," Phys. Rev., 109, No. 6, 1874, 1958.

Smith, R. L., "Propagation Characteristics of Whistlers Trapped in Field-Aligned Columns of Enhanced Ionization," J. Geophys. Res., 66, 3699, 1961, "Properties of the Outer Ionosphere Deduced from Nose Whistlers," J. Geophys. Res., 66, 3709, 1961.

Spitzer, L., "Physics of Fully Ionized Gases," Interscience, 78, 1956.

Storey, L. R. O., "An Investigation of Whistling Atmospherics," Phil. Trans. Roy. Soc. of London, A246, 113, 1953.

Thompson, W. B., "An Introduction to Plasma Physics," Addison-Wesley Publishing Co., 1962.

Van Allen, J. A., "Dynamics, Composition and Origin of the Geomagnetically-Trapped Corpuscular Radiation," Transactions of International Astronomical Union, XIB, 99, 1962.

List of Figures

Fig. 1 Whistler time-delay curves, computed from equation (35), assuming plasma number-density proportional to the Earth's magnetic field strength.

Fig. 2 Hose-instability curves for low-energy and high-energy plasma. Instability occurs in the equatorial plane, for any given L number, when n_0 exceeds the indicated value of n_0^*.

Fig. 3a Variation of pressure, density and temperature along the line of force L = 1.5 in an adiabatic protonosphere. Also shown, for comparison, are the variation of the Earth's magnetic field strength and number-density derived by ELS (1964).

Fig. 3b Variation of pressure, density and temperature along the line of force L = 3 in an adiabatic protonosphere.

Fig. 3c Variation of pressure, density and temperature along the line of force L = 6 in an adiabatic protonosphere.

Fig. 3d Variation of pressure, density and temperature along the polar line of force in an adiabatic protonosphere.

Fig. 4a Variation of pressure and density along the line of force L = 1.5 in an isothermal protonosphere.

Fig. 4b Variation of pressure and density along the line of force L = 3.0 in an isothermal protonosphere.

Fig. 4c Variation of pressure and density along the line of force L = 6.0 in an isothermal protonosphere.

Fig. 5a Normalized plasma density as a function of geomagnetic colatitude at a geocentric distance of 1.2 Earth radii for an adiabatic protonosphere.

Fig. 5b Normalized plasma density as a function of geomagnetic colatitude at a geocentric distance of 2.0 Earth radii for an adiabatic protonosphere.

Fig. 5c Normalized plasma density as a function of geomagnetic colatitude at a geocentric distance of 3.0 Earth radii for an adiabatic protonosphere.

Fig. 6 Azimuthal current density in equatorial plane (model adiabatic protonosphere).

Fig. 7 Distribution of azimuthal current density along given lines of force (model adiabatic protonosphere).

Fig. 8a Variation of pressure, density and temperature along the ling of force L = 1.5 in an adiabatic radiation belt.

Fig. 8b Variation of pressure, density and temperature along the line of force L = 3.0 in an adiabatic radiation belt.

Fig. 8c Variation of pressure, density and temperature along the line of force L = 6.0 in an adiabatic radiation belt.

Fig. 9a Variation of pressure and density along the line of force L = 1.5 in an isothermal radiation belt.

Fig. 9b Variation of pressure and density along the line of force L = 3.0 in an isothermal radiation belt.

Fig. 9c Variation of pressure and density along the line of force L = 6.0 in an isothermal radiation belt.

Fig. 10a Isobaric contours in polar coordinates. Units for P are in dyn/cm^2. Heavy line is the magnetic line of force for L = 6 (model adiabatic radiation belt).

Fig. 10b Isobaric contours in polar coordinates. Units for P are in dyn/cm^2. Heavy line is the magnetic line of force for L = 6 (model adiabatic radiation belt).

Fig. 10c Contours of constant density. Units are in gm/cm^3. Heavy line is the magnetic line of force for L = 6 (model adiabatic radiation belt).

Fig. 10d Contours of constant current density. Units are in $statamp/cm^2$. Westward current is shown as solid line, eastward current shown as broken line. Heavy line is the magnetic line of force for L = 6 (model adiabatic radiation belt).

Fig. AA-1 Dipole coordinates

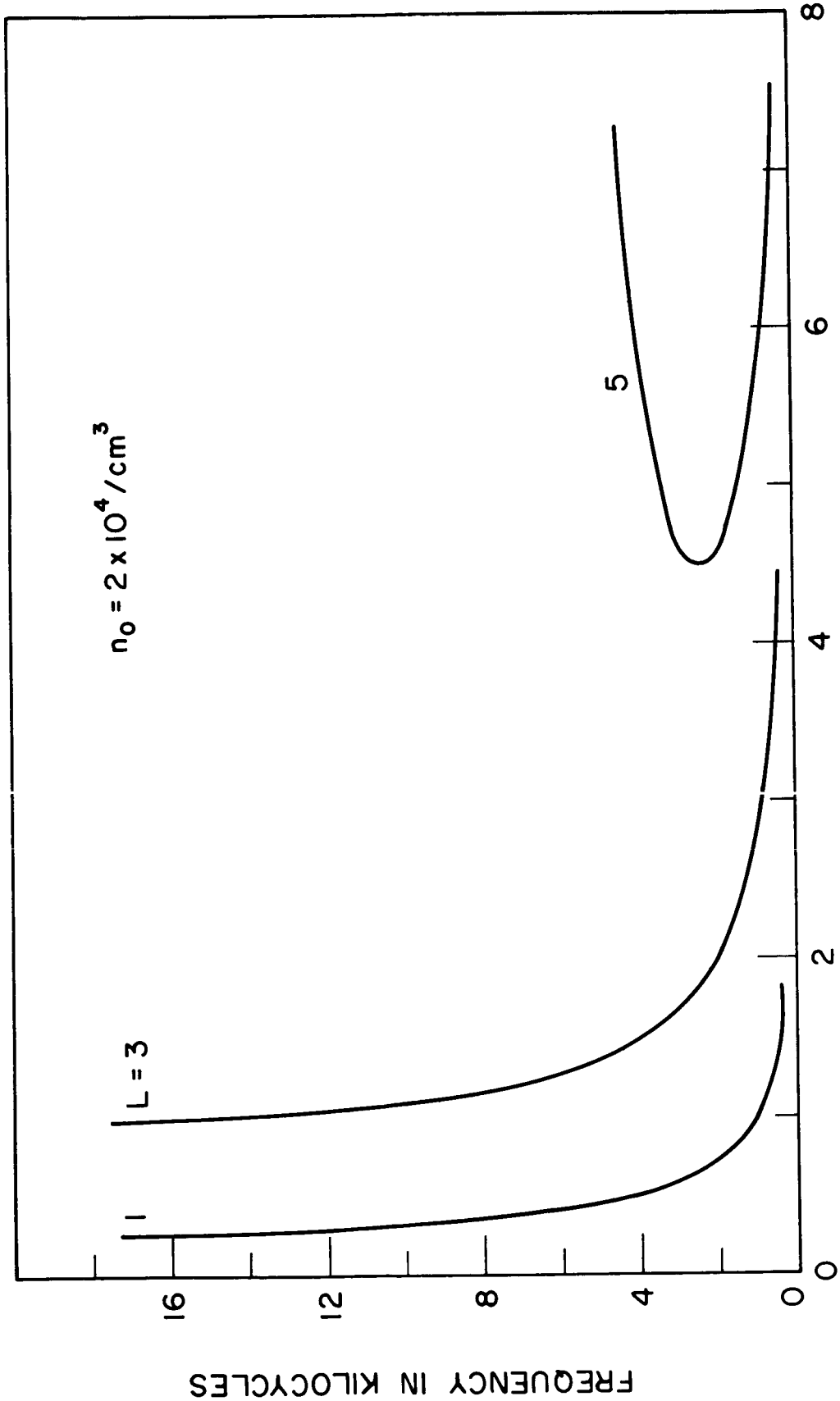
$n_0 = 2 \times 10^4/cm^3$
L = 3
1
5
0
2
4
6
8
0
4
8
12
16
TIME DELAY IN SECONDS
FREQUENCY IN KILOCYCLES

Figure 1

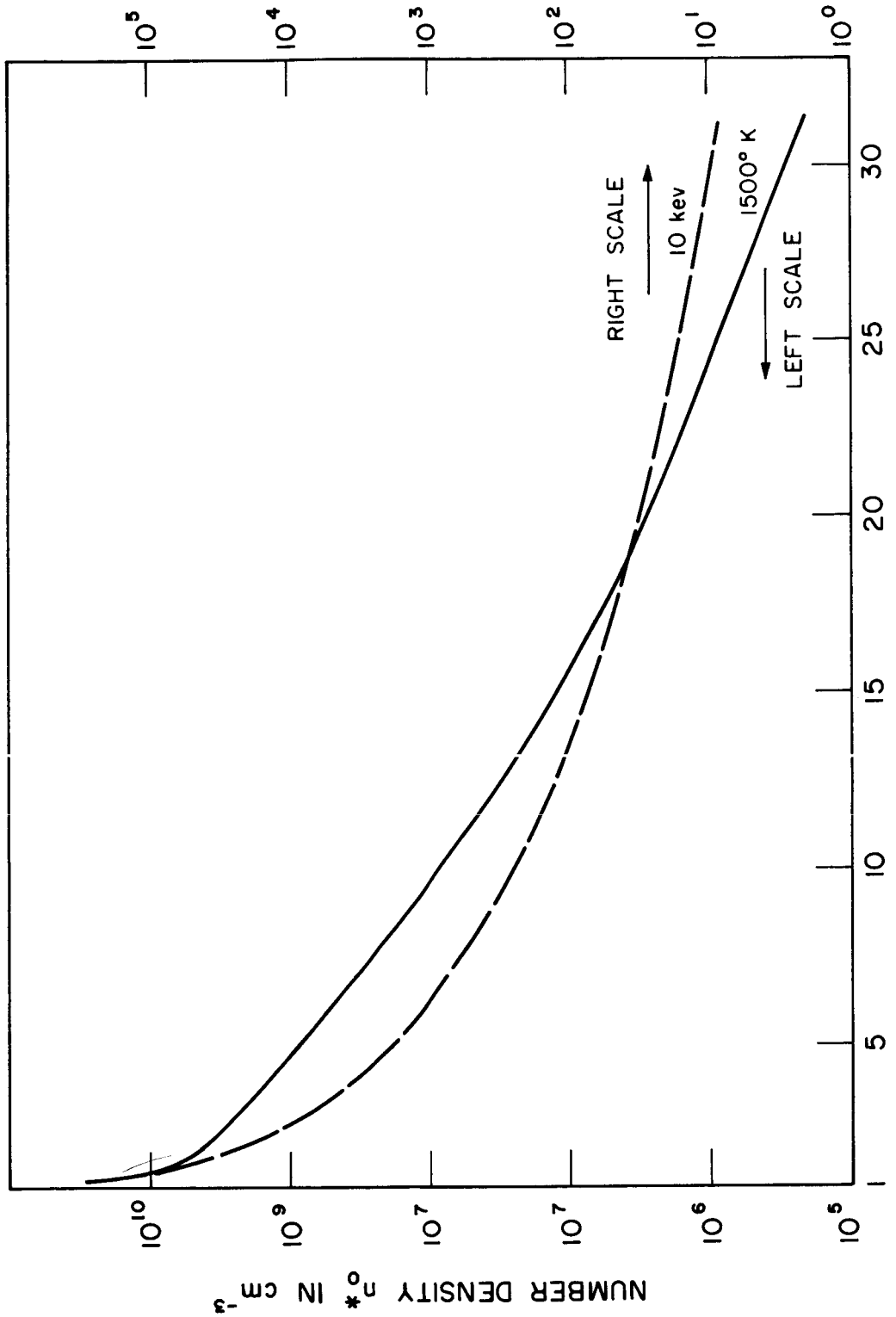
NUMBER DENSITY n_o^* IN cm^{-3}
10^{10}
10^9
10^7
10^7
10^6
10^5
10^5
10^4
10^3
10^2
10^1
10^0
1
5
10
15
20
25
30
L VALUES
RIGHT SCALE
10 kev
1500° K
LEFT SCALE

Figure 2

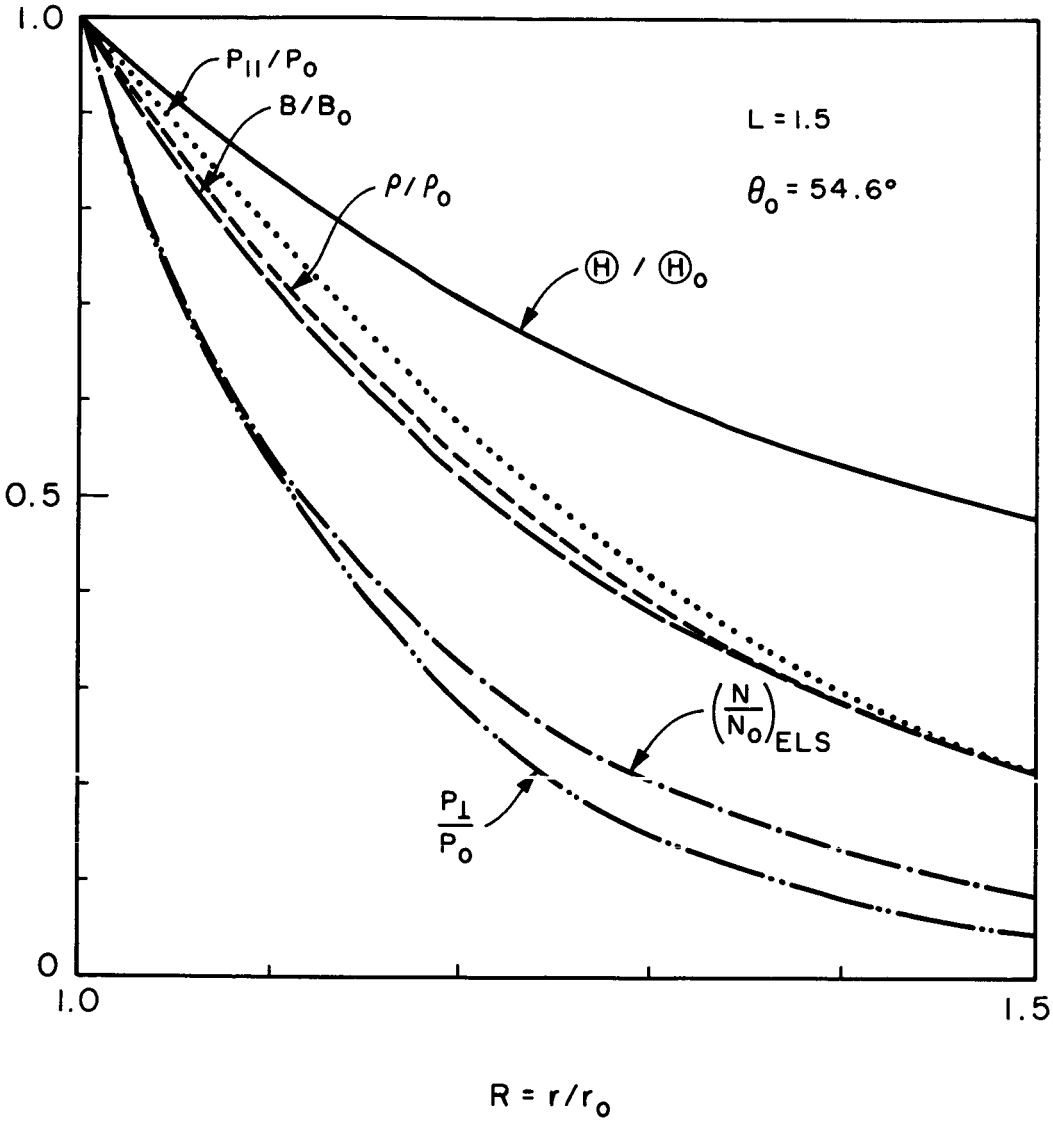
1.0
0.5
0
1.0
1.5
P_{11}/P_0
B/B_0
ρ/ρ_0
$\textcircled{H}/\textcircled{H}_0$
L = 1.5
$\theta_0 = 54.6°$
$\left(\frac{N}{N_0}\right)_{ELS}$
$\frac{P_\perp}{P_0}$
$R = r/r_0$

Figure 3a

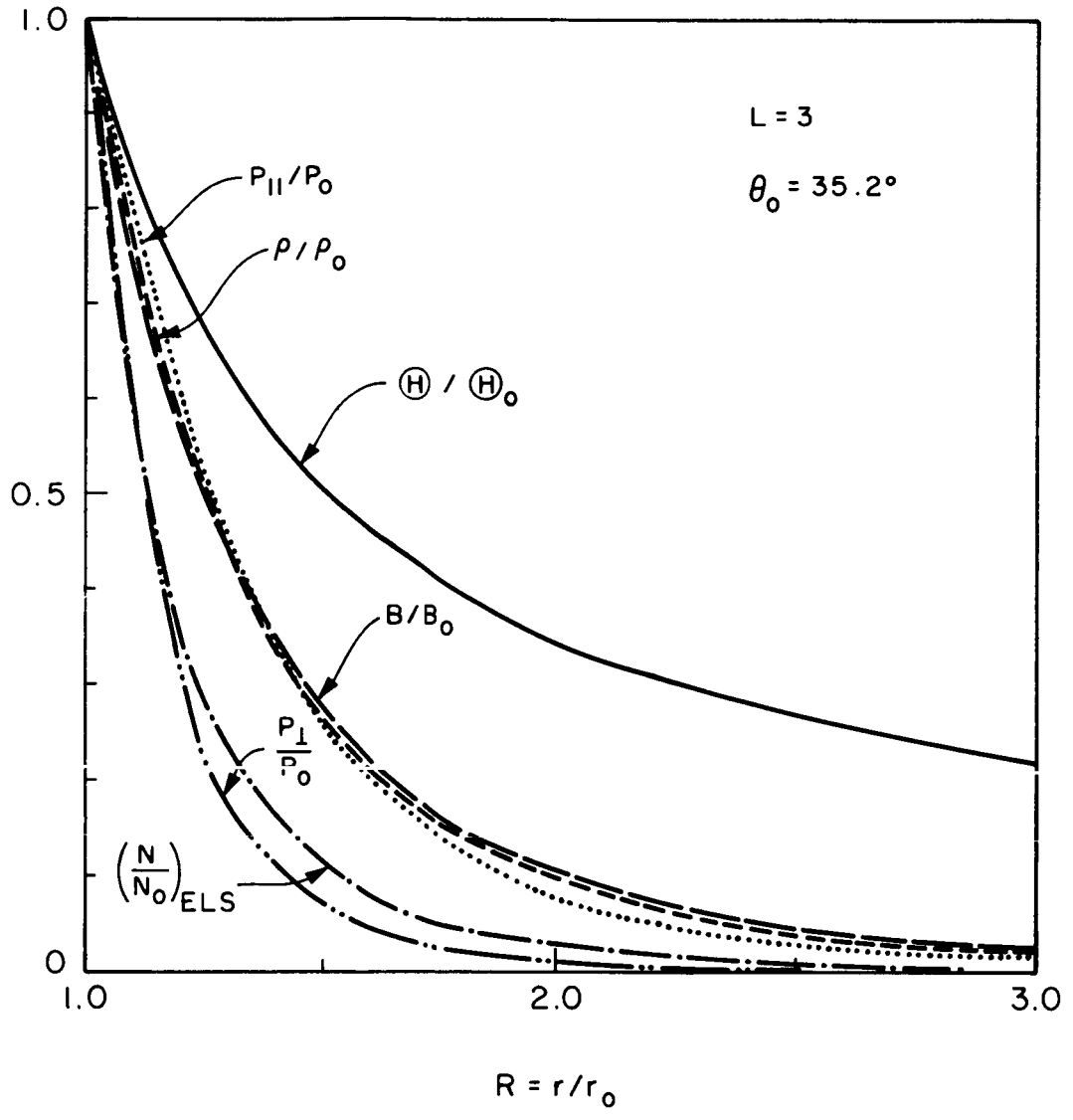
1.0
0.5
0
1.0
2.0
3.0
L = 3
$\theta_0 = 35.2°$
P_{II}/P_0
ρ/ρ_0
$\textcircled{H}/\textcircled{H}_0$
B/B_0
$\frac{P_\perp}{P_0}$
$\left(\frac{N}{N_0}\right)_{ELS}$
$R = r/r_0$

Figure 3b

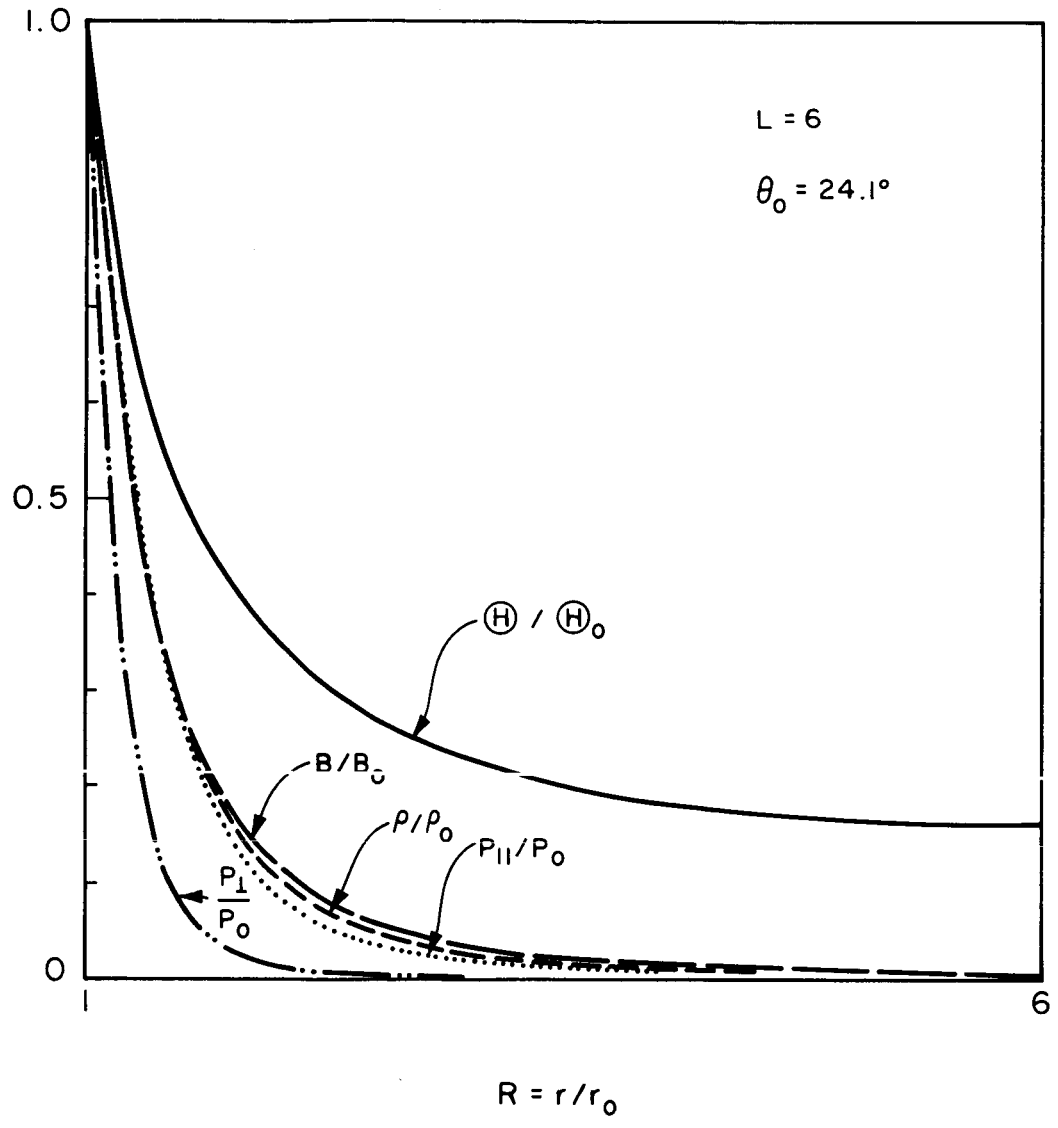

Figure 3c

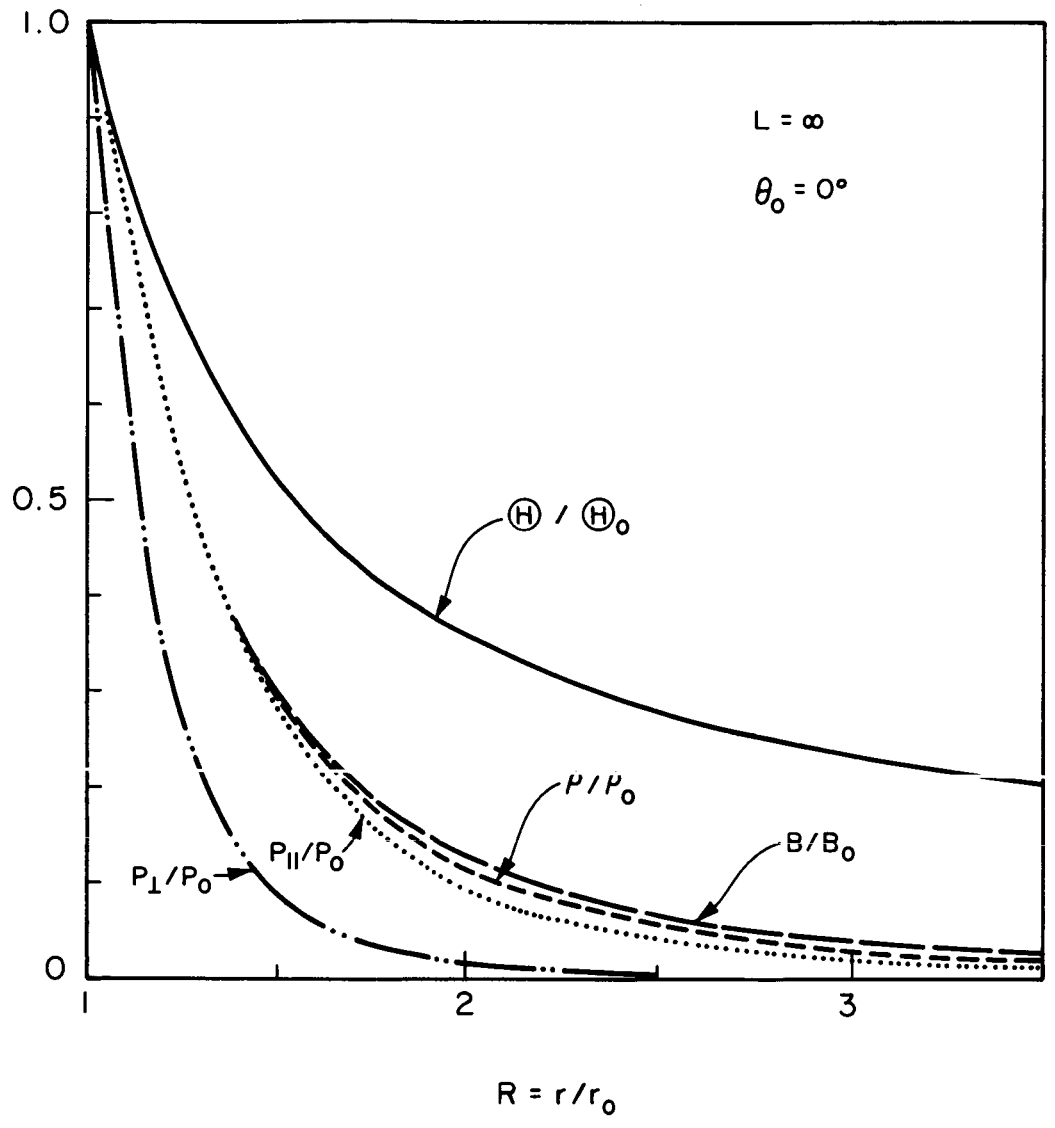

Figure 3d

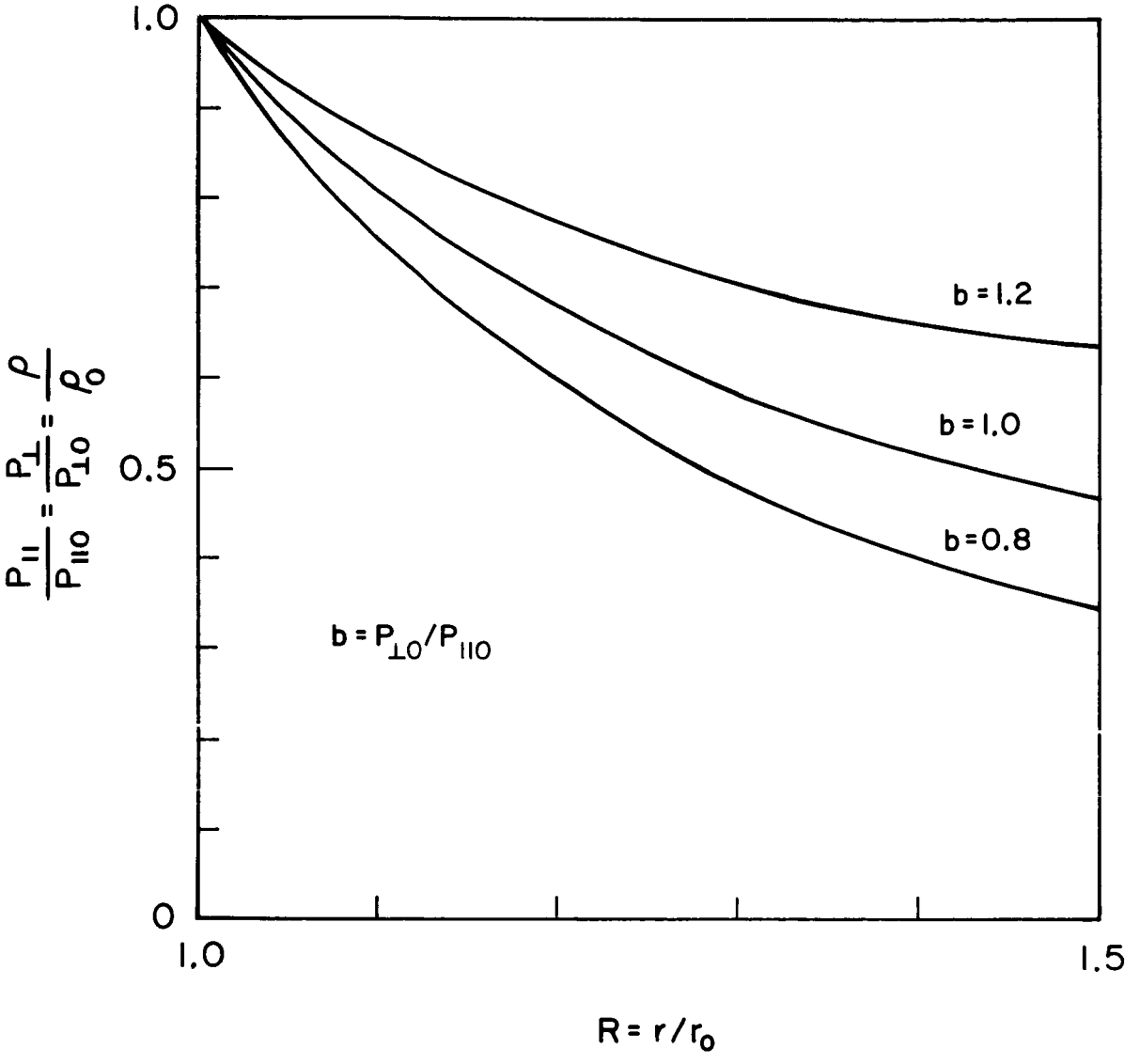
1.0
0.5
0
1.0
1.5
$\frac{P_{11}}{P_{110}} = \frac{P_\perp}{P_{\perp 0}} = \frac{\rho}{\rho_0}$
$R = r/r_0$
b = 1.2
b = 1.0
b = 0.8
$b = P_{\perp 0}/P_{110}$

Figure 4a

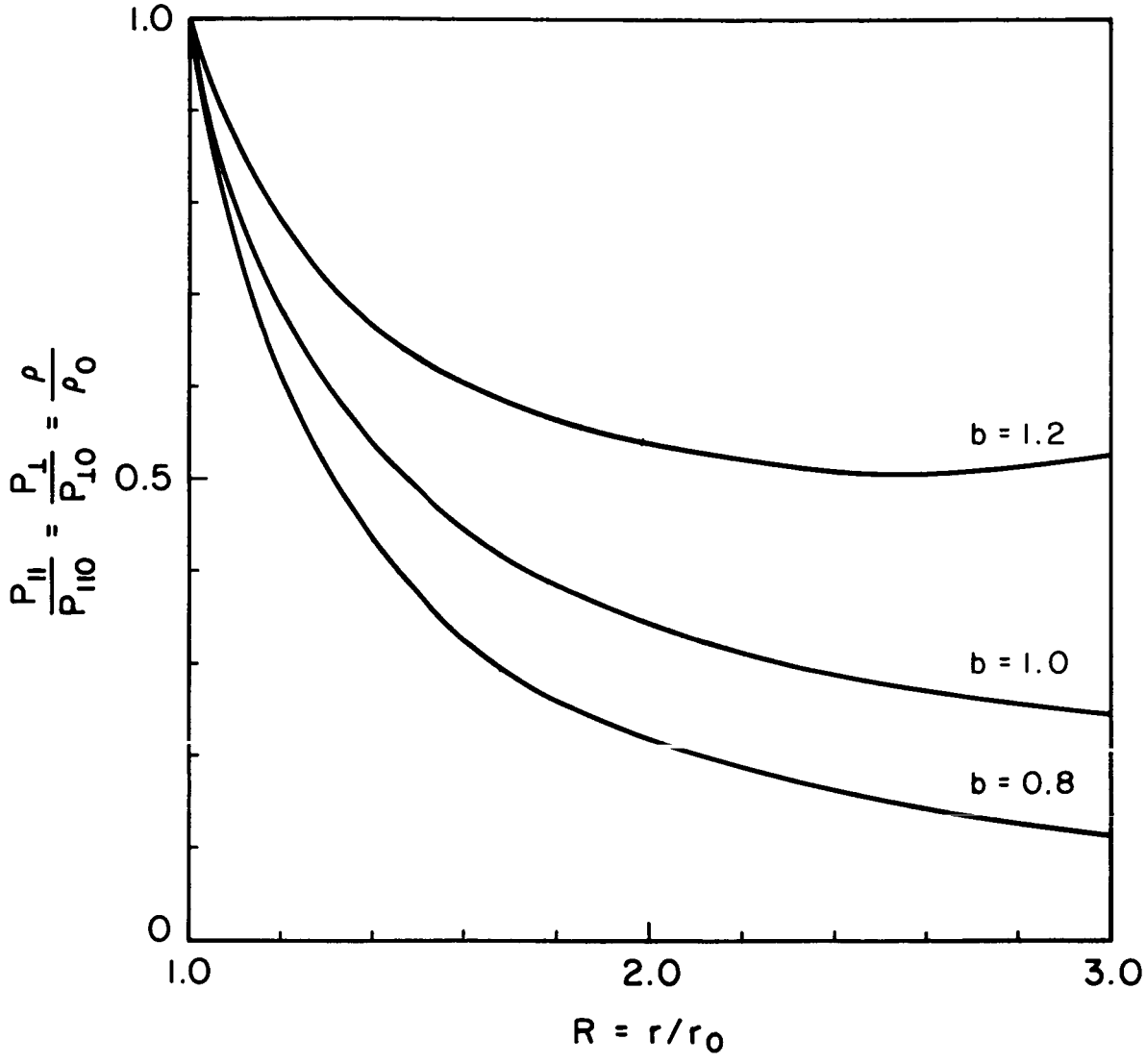
1.0
0.5
0
1.0
2.0
3.0
$\frac{P_{11}}{P_{110}} = \frac{P_{\perp}}{P_{\perp 0}} = \frac{\rho}{\rho_0}$
$R = r/r_0$
b = 1.2
b = 1.0
b = 0.8

Figure 4b

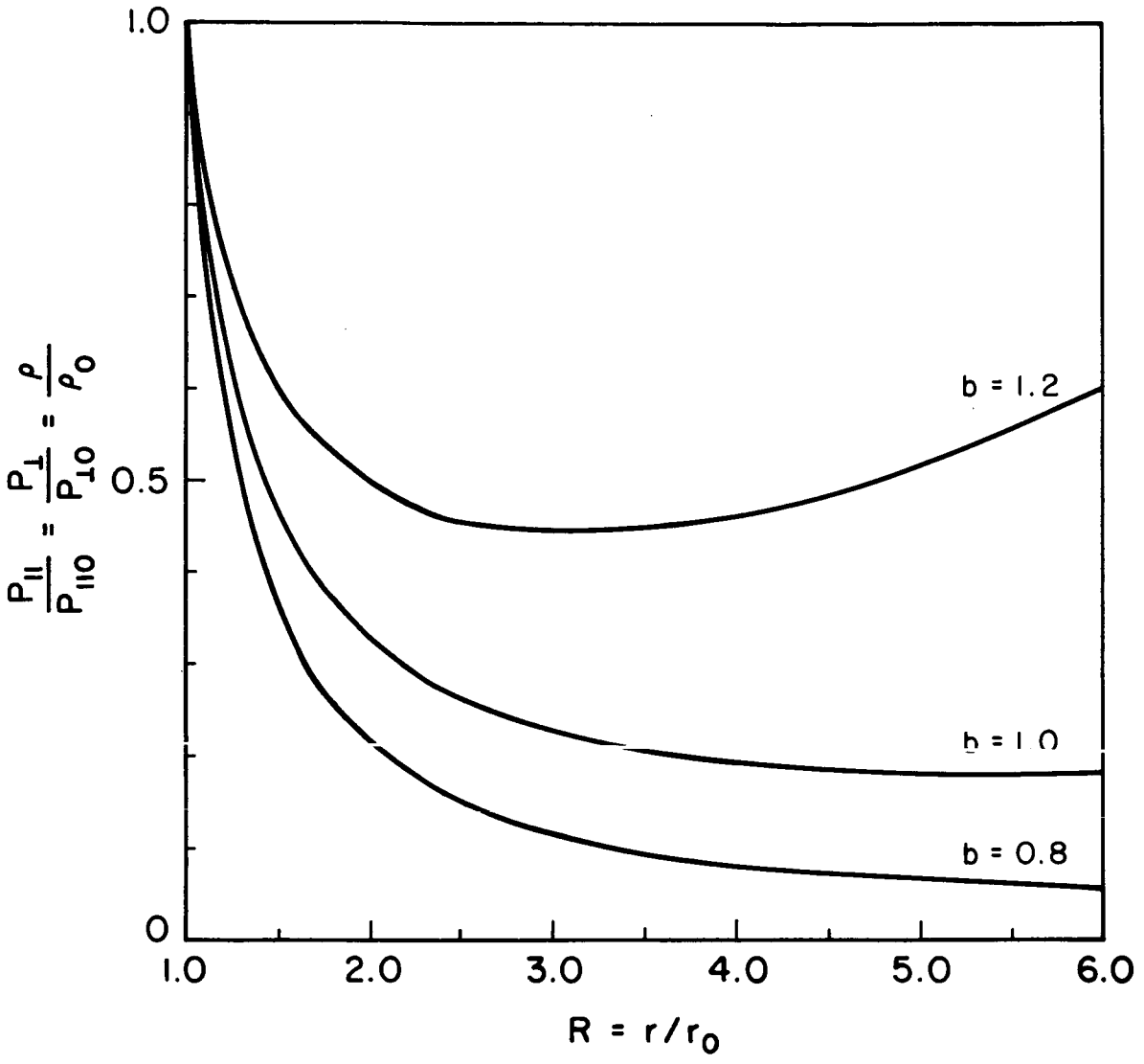
1.0
0.5
0
1.0
2.0
3.0
4.0
5.0
6.0
b = 1.2
b = 1.0
b = 0.8
$\frac{P_{11}}{P_{110}} = \frac{P_{\perp}}{P_{\perp 0}} = \frac{\rho}{\rho_0}$
$R = r/r_0$

Figure 4c

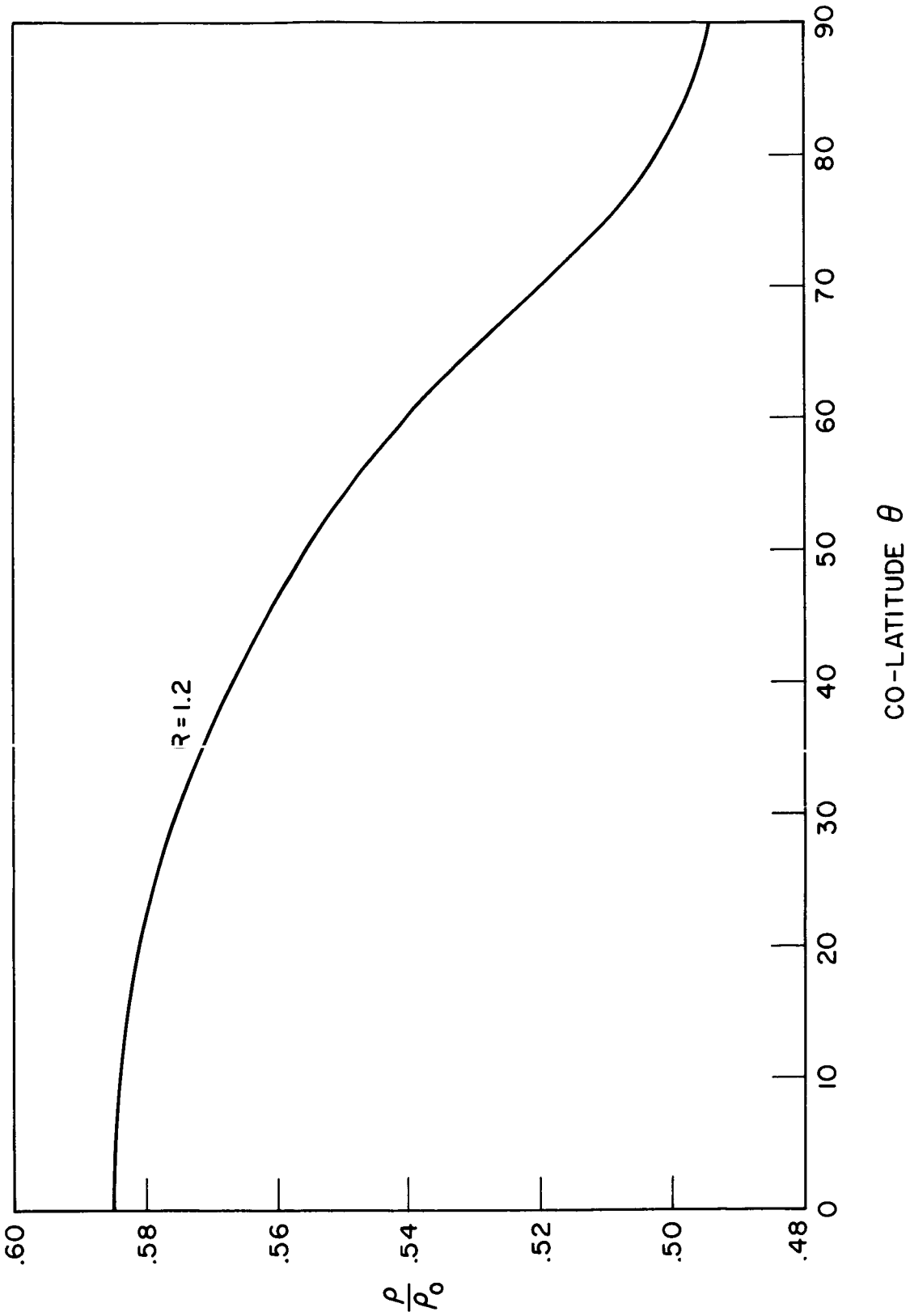
R=1.2
.60
.58
.56
.54
.52
.50
.48
$\frac{\rho}{\rho_0}$
0
10
20
30
40
50
60
70
80
90
CO-LATITUDE θ

Figure 5a

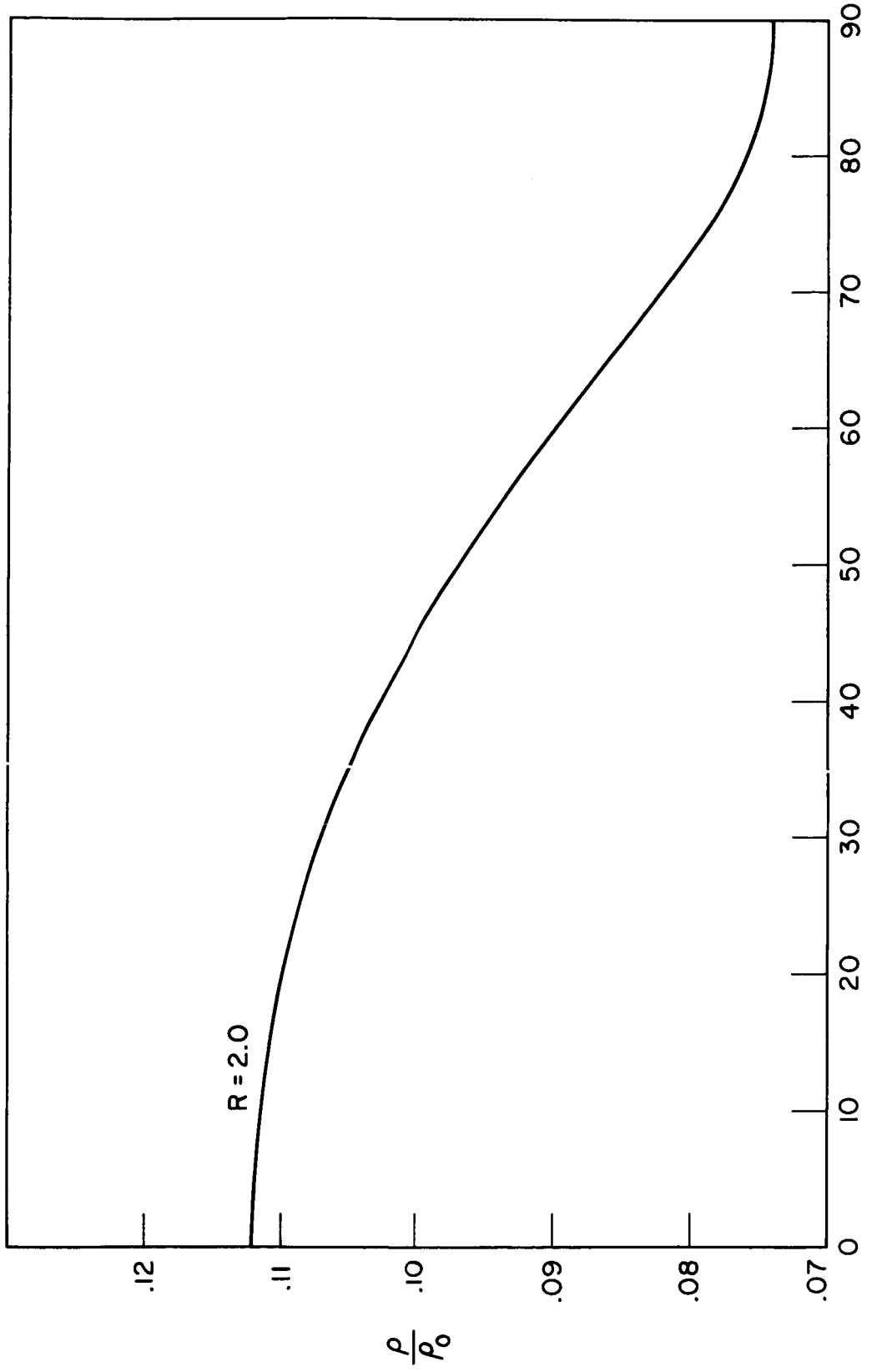
R = 2.0
.12
.11
.10
.09
.08
.07
$\frac{\rho}{\rho_0}$
0
10
20
30
40
50
60
70
80
90
CO-LATITUDE θ

Figure 5b

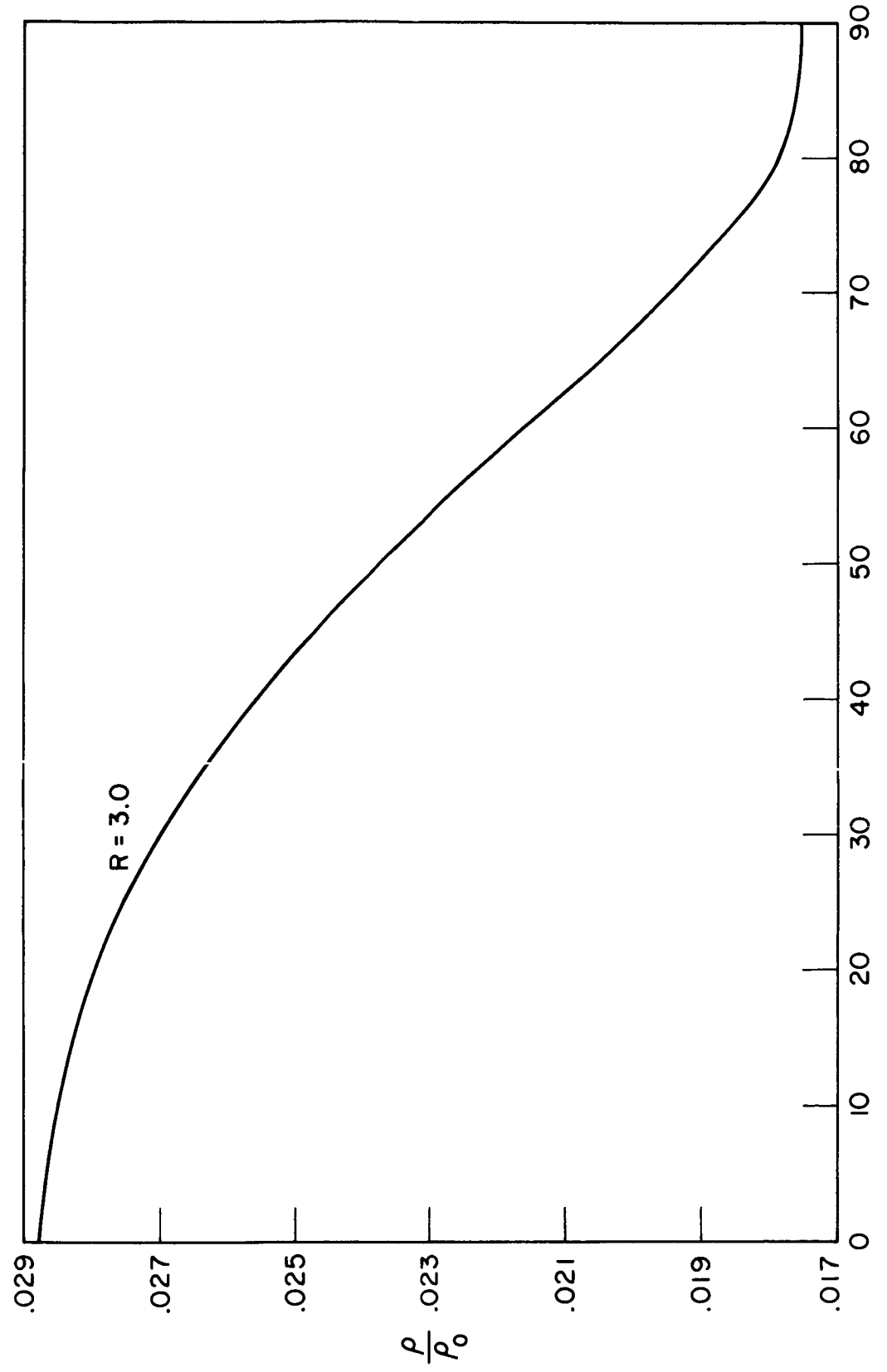
R = 3.0
.029
.027
.025
.023
.021
.019
.017
$\frac{\rho}{\rho_0}$
0
10
20
30
40
50
60
70
80
90
CO-LATITUDE θ

Figure 5c

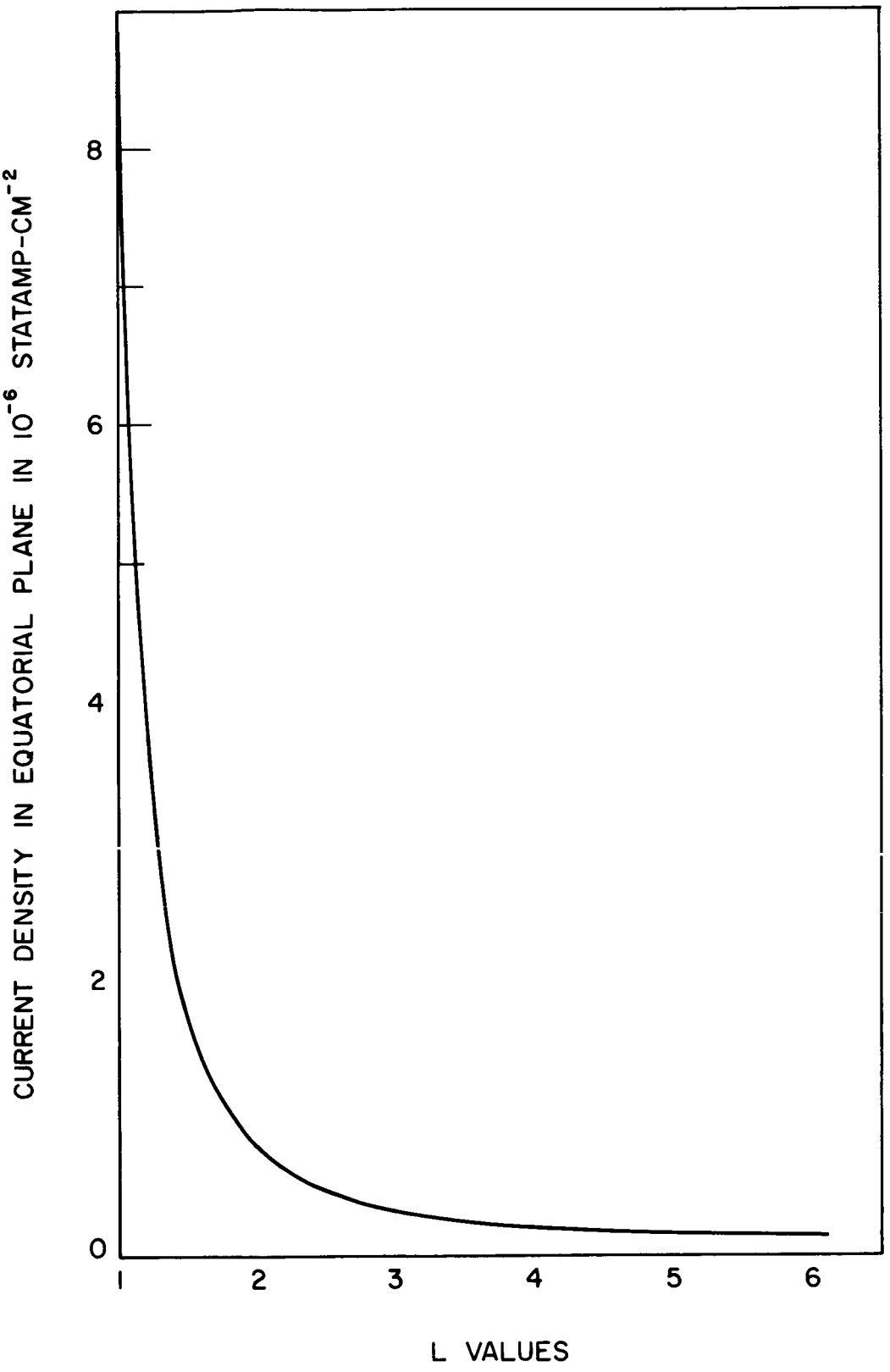
CURRENT DENSITY IN EQUATORIAL PLANE IN 10^{-6} STATAMP-CM^{-2}
8
6
4
2
0
1
2
3
4
5
6
L VALUES

Figure 6

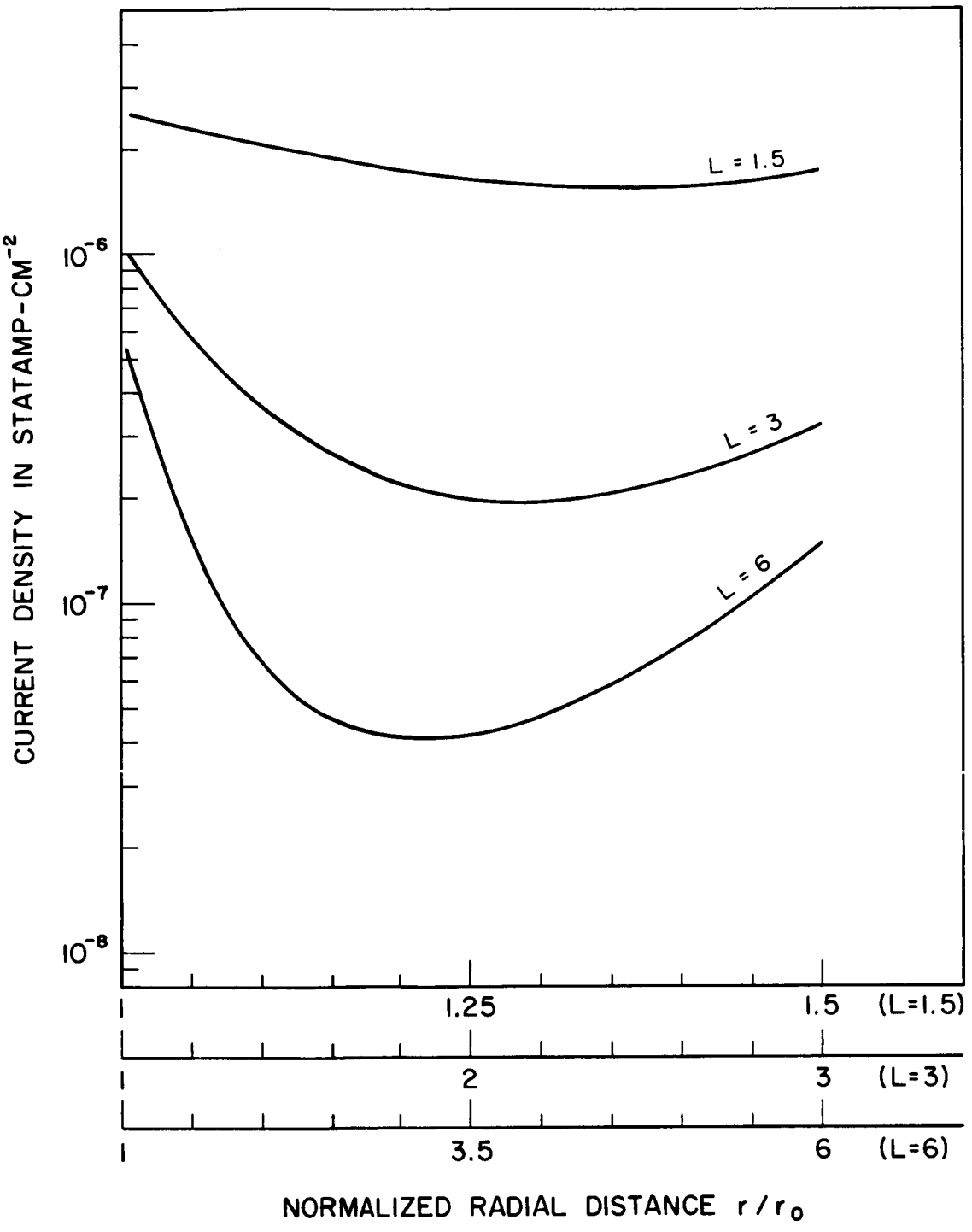
CURRENT DENSITY IN STATAMP-CM^{-2}
10^{-6}
10^{-7}
10^{-8}
L = 1.5
L = 3
L = 6
1
1.25
1.5
(L=1.5)
1
2
3
(L=3)
1
3.5
6
(L=6)
NORMALIZED RADIAL DISTANCE r / r_0

Figure 7

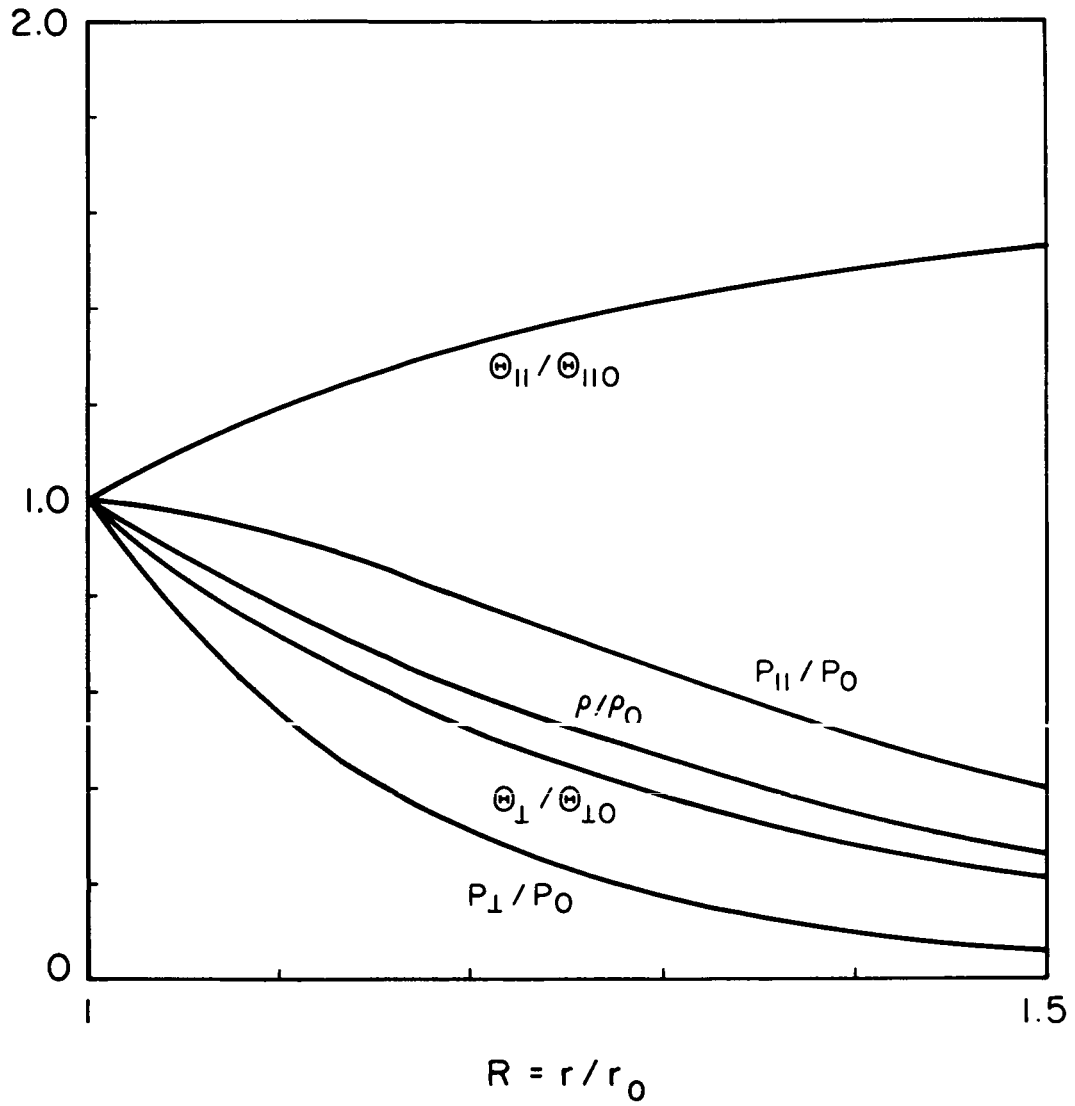
2.0
1.0
0
1
1.5
$\Theta_{11} / \Theta_{110}$
P_{11} / P_0
ρ / ρ_0
$\Theta_{\perp} / \Theta_{\perp 0}$
$P_{\perp} / P_0$
$R = r / r_0$

Figure 8a

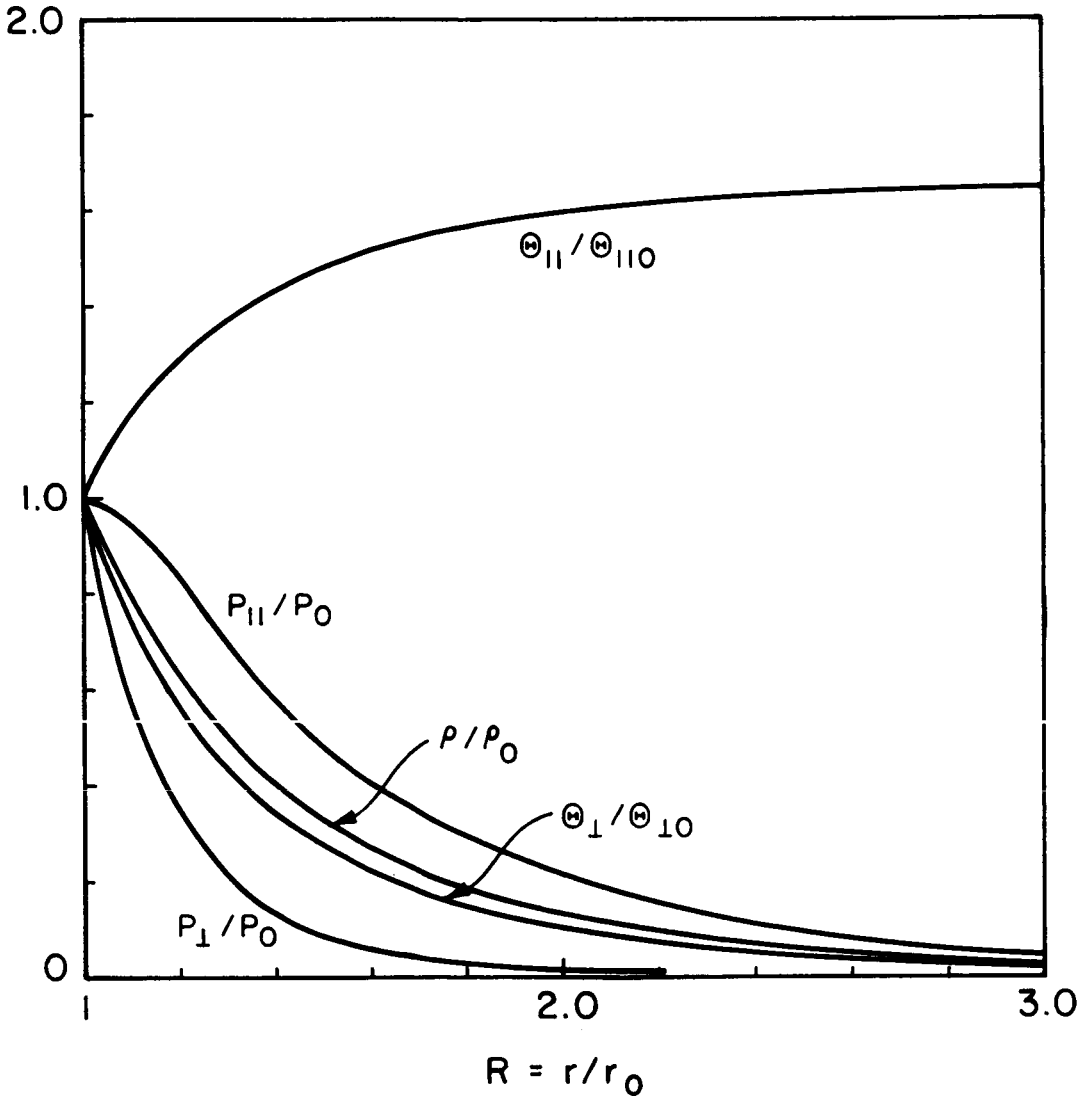
2.0
1.0
0
1
2.0
3.0
Θ_{11}/Θ_{110}
P_{11}/P_0
ρ/ρ_0
$\Theta_\perp/\Theta_{\perp 0}$
$P_\perp/P_0$
$R = r/r_0$

Figure 8b

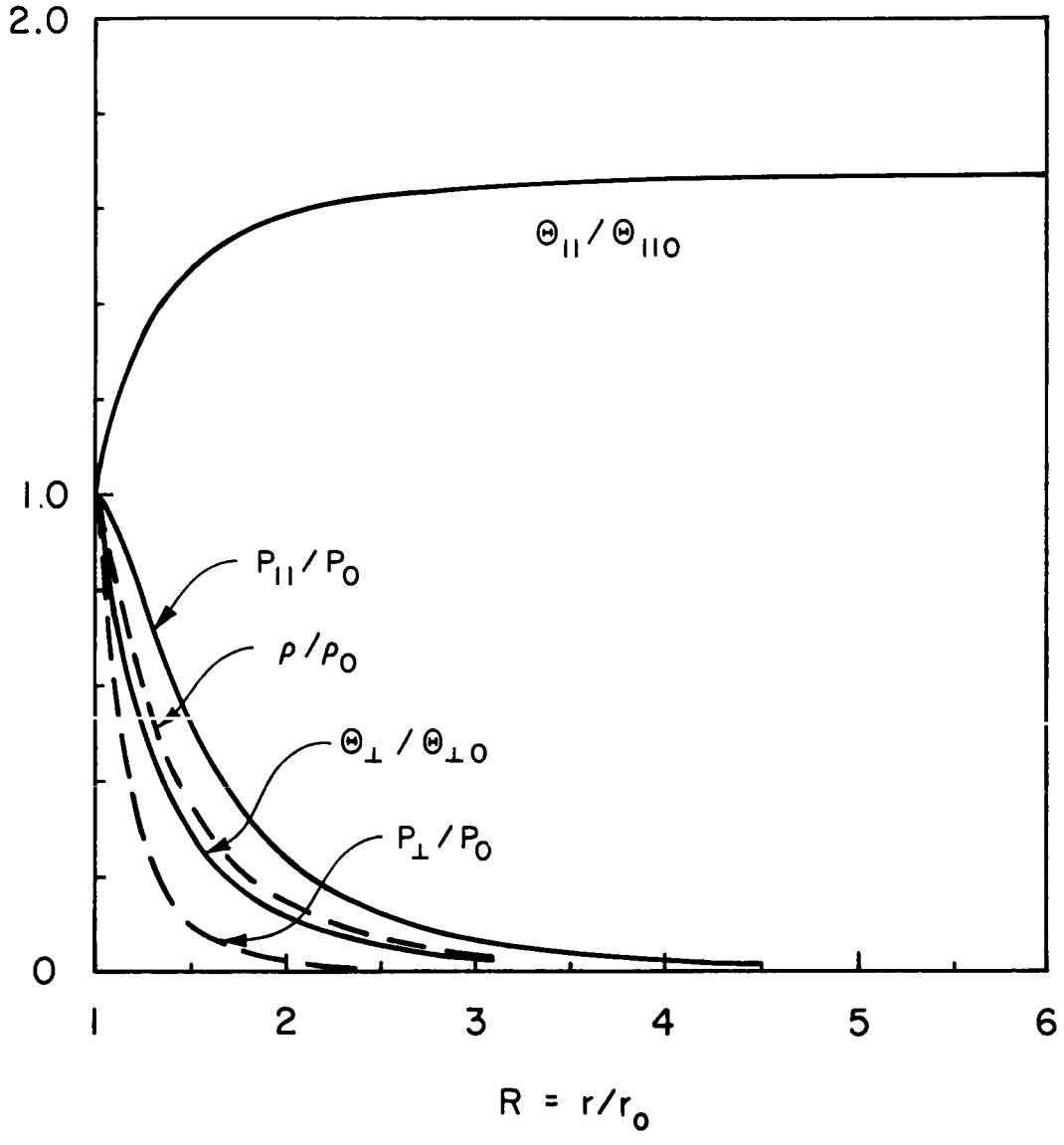
2.0
1.0
0
1
2
3
4
5
6
Θ_{11}/Θ_{110}
P_{11}/P_0
ρ/ρ_0
$\Theta_\perp/\Theta_{\perp 0}$
$P_\perp/P_0$
$R = r/r_0$

Figure 8c

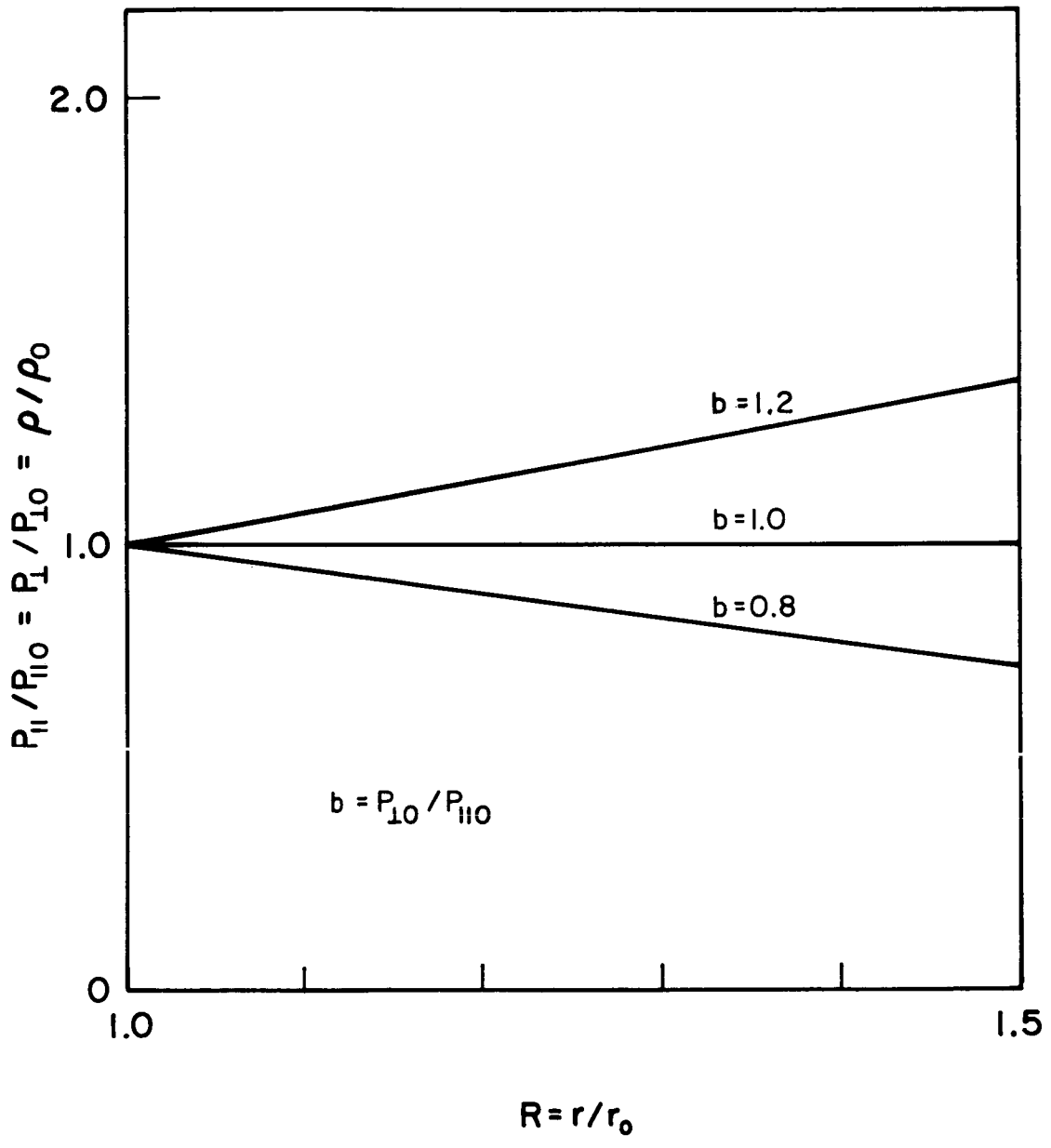
2.0
1.0
0
1.0
1.5
$P_{11}/P_{110} = P_{\perp}/P_{\perp 0} = \rho/\rho_0$
b = 1.2
b = 1.0
b = 0.8
$b = P_{\perp 0}/P_{110}$
$R = r/r_0$

Figure 9a

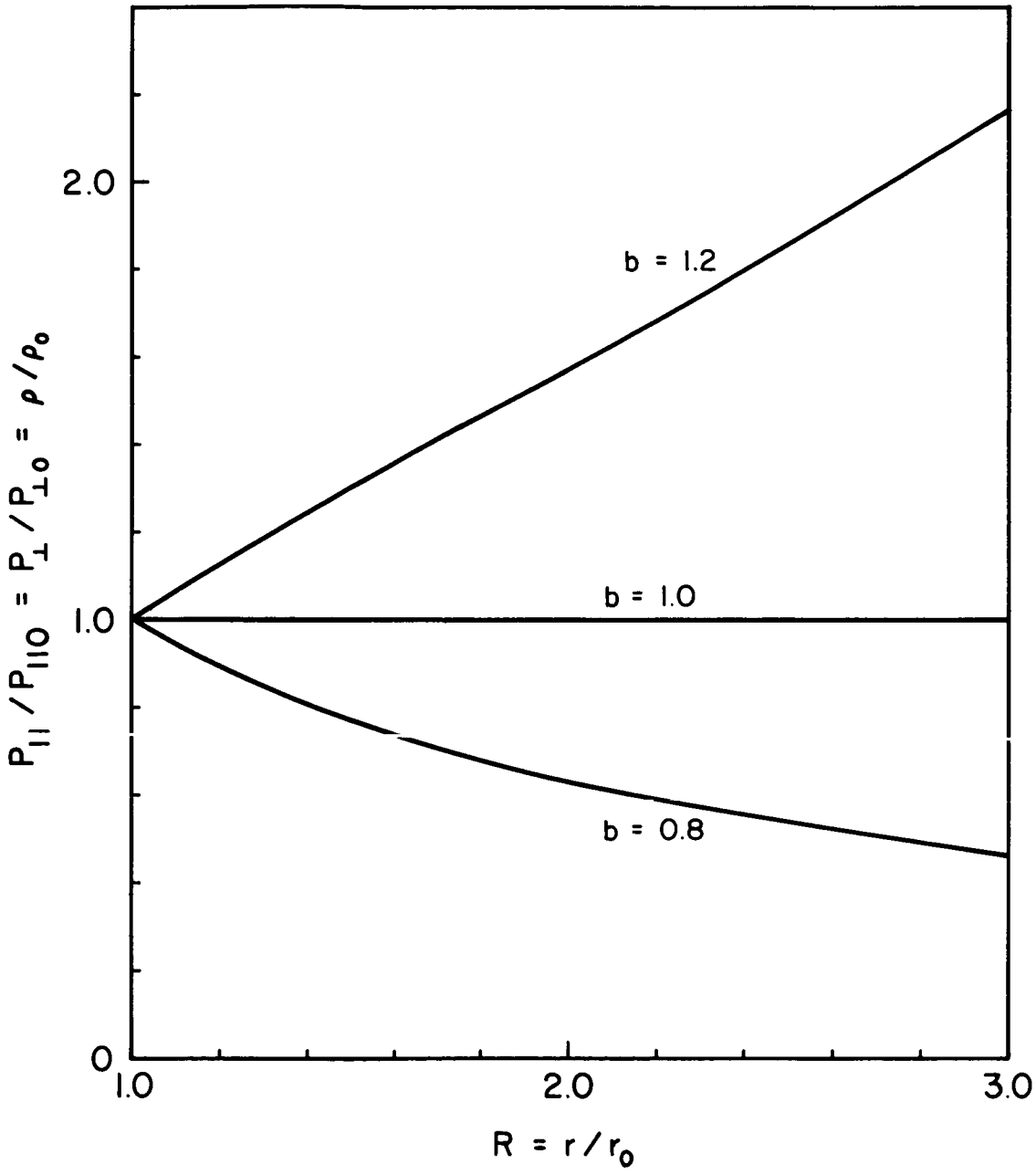

Figure 9b

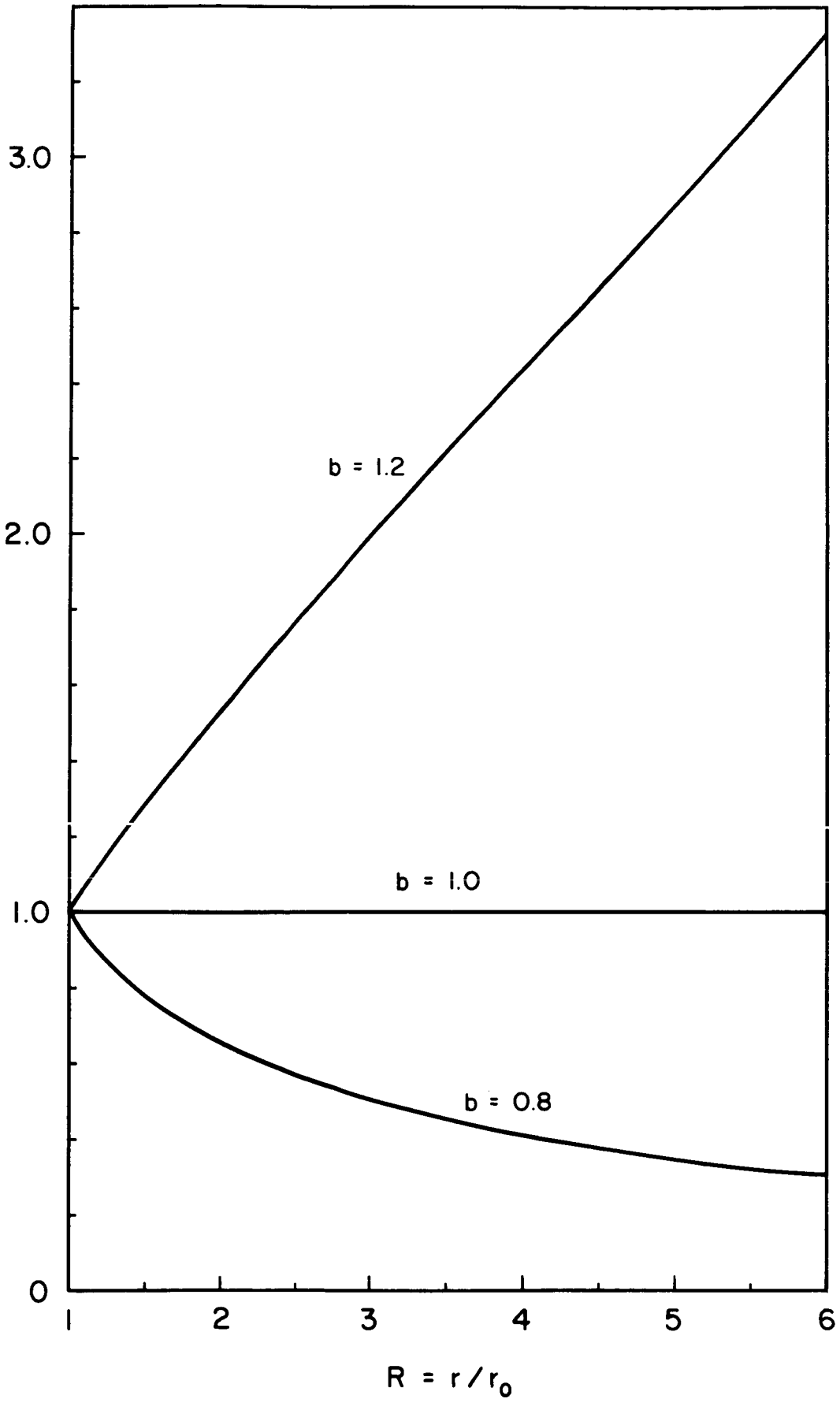

Figure 9c

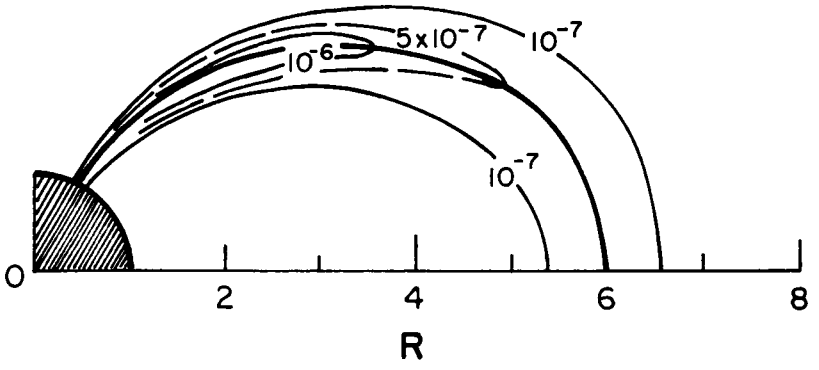

Figure 10a

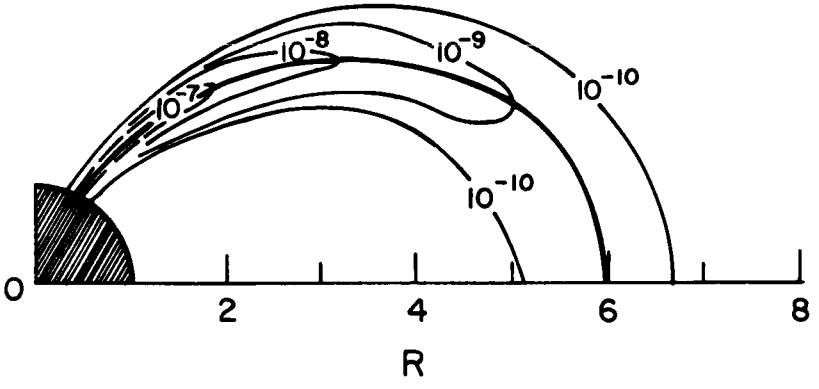

Figure 10b

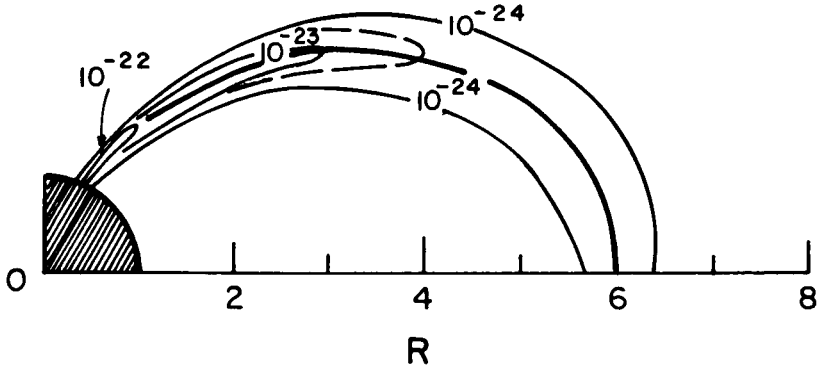

Figure 10c

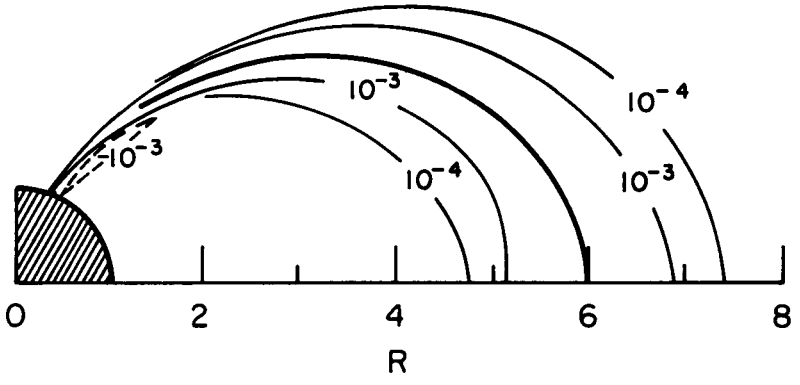

Figure 10d

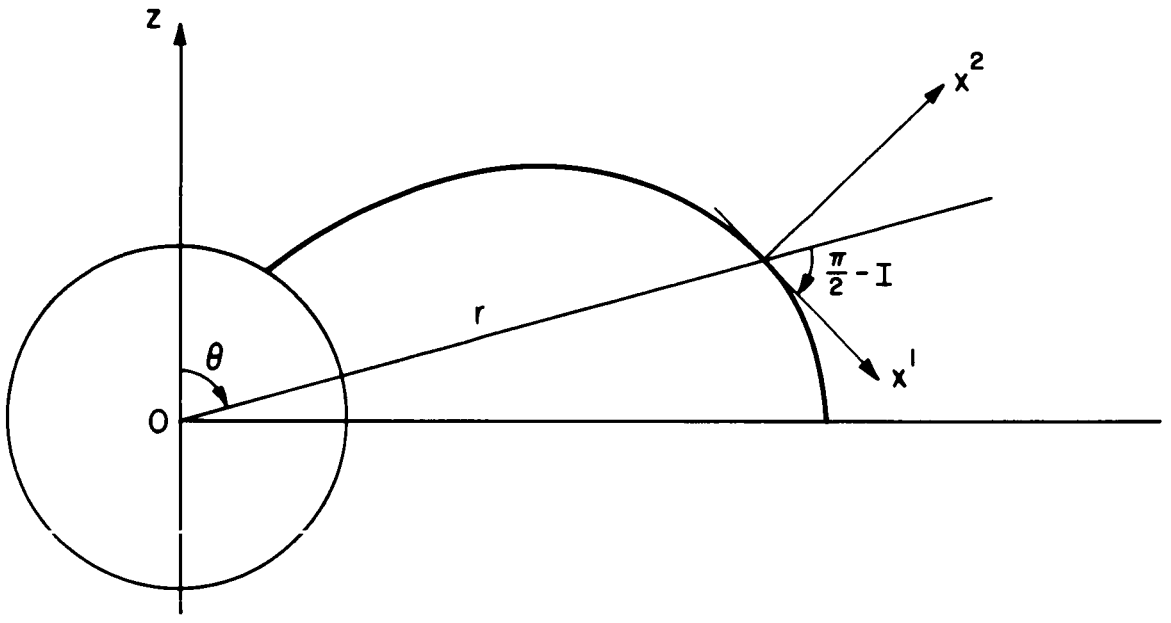

Figure AA-1